Vacuum-Assisted Wet Shaping of Paper

A Thesis
Presented to
The Academic Faculty

by

Amanda J. Busch

In Partial Fulfillment
Of the Requirements for the Degree
Master of Science in Mechanical Engineering

School of Mechanical Engineering
Georgia Institute of Technology
May 2006

Vacuum-Assisted Wet Shaping of Paper

Approved by:

Dr. Fred Ahrens, Advisor
School of Mechanical Engineering
Georgia Institute of Technology

Dr. Timothy Patterson
School of Mechanical Engineering
Georgia Institute of Technology

Dr. David Rosen
School of Mechanical Engineering
Georgia Institute of Technology

Date Approved: April 7, 2006

ACKNOWLEDGEMENTS

Grateful acknowledgement is made for the valuable suggestions and guidance of my advisor, Fred Ahrens, and also to the members of my committee, Tim Patterson and David Rosen. Thanks also to James Loughran.

The financial support of the Institute of Paper Science and Technology and its member companies is also greatly appreciated.

TABLE OF CONTENTS

LIST OF TABLES

LIST OF FIGURES

LIST OF SYMBOLS AND ABBREVIATIONS

a	Radius
c	Constant of integration
D	Flexural rigidity
ε	Strain
E	Modulus of Elasticity
M_r	Radial Moment
M_θ	Tangential Moment
ν	Poisson's ratio
p	Pressure load
Q_r	Force (per unit length)
r	Radial Position
σ	Stress
SLA	Stereolithography
t	Thickness
TAD	Through Air Drying
VTH	Vacuum Test Head
w	Deflection

SUMMARY

Premium absorbent paper products (e.g., two-ply towel and tissue) can achieve higher fluid holding capacity per unit dry weight by means of increasing their void volume per unit weight. In turn, high void volume can be attained by increasing the overall thickness of each ply through molding the paper into a three-dimensional ("mini-egg-crate") structure before drying it.

This research investigates the effect of three types of parameters: mold geometrical, operational, and paper parameters. These variables are examined with respect to their effect on the resulting overall thickness. Because the experimental research is fundamental in nature, it employs molding structures of a simplified geometry (produced via rapid prototyping techniques) rather than the geometrically complex molding fabrics used commercially.

A goal of the project is the understanding of the physics of the wet shaping process, in which vacuum is used to deform the wet paper web into the openings in the molding structure. Another goal is identification of limitations or boundaries of the wet shaping process (e.g., conditions for which "pinholes" occur in the paper). Supporting theoretical analysis of the shaping/molding problem is performed, to provide bases for correlating experimental data and for the optimization of molding geometrical parameters. The result of this study provides quantitative information for some variables that affect the final sheet thickness.

1 INTRODUCTION

Modern industrialized societies hardly think twice about the quantity of disposable paper products that are in constant use. Naturally, because of the wide use, manufacturing of such products has become one of the largest industries in these nations and because of such demand, development of improved versions of these products and their manufacturing methods has increased.

Disposable paper products (e.g., two-ply towel and tissue) are made from one or more webs of tissue paper. If the products are to meet consumer performance demands, they must exhibit certain physical characteristics, including high strength, sufficient softness, and good absorbency.

Premium absorbent paper products can achieve higher absorbency per unit dry weight by means of increasing their void volume per unit weight. In turn, high void volume can be attained by increasing the overall thickness of each ply through molding the paper into a three-dimensional ("mini-egg-crate") structure before drying it.

This research investigates the effects of three different types of parameters on thickness. These are mold geometrical, operational, and paper parameters. Mold geometrical parameters include such variables as size and shape of the mold pattern. Because the experimental research is fundamental in nature, it employs molding structures of a simplified geometry (produced via rapid prototyping techniques) rather than the

geometrically complex molding fabrics used commercially. Effects of molding process variables, such as vacuum level, on the resulting overall thickness are investigated. Paper parameters such as initial paper moisture content are the final category of variables studied.

This paper considers several examples of these parameters. Not only does it consider a parameter's immediate effect, but also it investigates the interrelation between various parameters. These parameters are investigated with regard to their effect on the final sample thickness. An attempt to relate the thickness results to a simple theoretical model is provided.

2 LITERATURE REVIEW

Papermaking has often been considered an art form. However, with the large demand and the mass production needed to supply product for such demand, papermaking has also become a highly optimized science. Especially in the competitive area of absorbent paper products, modern companies have realized the need for optimization of products along with increased aesthetic properties.

2.1 Decorative Formation of Tissue by Directing Flow through Forming Fabric

One way in which the aesthetic aspect of papermaking is infused with science is through the formation of the paper sheets on the forming fabric. In one invention, there is a decorative forming fabric for the papermaking, which has areas of slower drainage that define distinct decorative patterns. To obtain these patterns in the finished sheet, the pulp solution is comprised of a mixture of long and short papermaking fibers. A solution of about 50 percent dry weight short fibers and at least 20 percent dry weight long fibers allows the short fibers to flow around the decorative design areas[1]. This concentrates the short fibers in the high flow rate areas and allows the long fibers to bridge the decorative, slower flow rate areas producing a varied basis weight decorative paper.

2.2 Shaping Processes

2.2.1 Through Air Drying (TAD) Process

The through air drying, or TAD, process is the predominant way of creating today's premium absorbent paper products. Products created via TAD are the consumer's choice

due to the increased product characteristics of softness, strength and absorbency that TAD can produce.

The TAD process is one of the most effective methods for increasing bulk and softness in absorbent paper products. While conventional tissue machines press the paper sheet onto a Yankee cylinder, TAD technology removes water by pulling high temperature air through the sheet after it has been shaped, or molded, using a special TAD fabric.

These TAD papermaking processes generally take multiple steps. First, the watery dispersion of papermaking fibers is molded into a web on a forming fabric. Next, the web is transferred to a deflection member (shaping fabric), which has a patterned network surface defining many deflection conduits. Water from the web is removed as the papermaking fibers are deflected (via vacuum) into the network surface. The web is then at least partially dried via hot air through-flow while it is still embedded in the shaping fabric. This web is then transferred to a Yankee dryer cylinder and creped if desired.

As shown in Figure 2.1, the simplified through air dryer includes a cylindrical deck (1) supported by a pair of opposing heads (2). These heads are mounted on a rotating shaft (3) surrounded by a pair of bearings (4)[2].

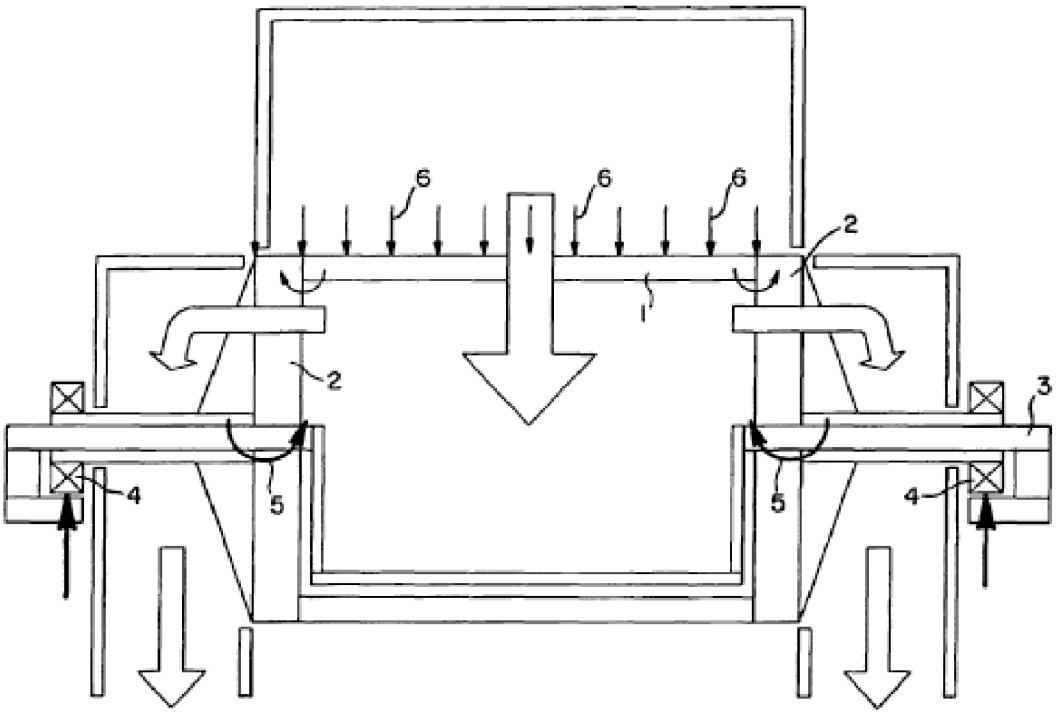

Figure 2.1 – Simplified Diagram of a TAD Machine[2]

The TAD technology keeps the paper from becoming as compressed as in traditional manufacture, which helps explain why the TAD sheet has up to 75% more bulk than a conventional sheet of the same weight[3]. Not only does the TAD process increase the bulk, it also increases the texture. With this, various shapes and decorative patterns can be added to the final product, enhancing the aesthetic appeal.

Although Figure 2.1 is only a simplified diagram, it identifies some of the difficulties found in these standard TAD machines. The bearings must be a significant distance from the opposing heads to prevent exposure to the hot gas flow. As a result of this placement, moments (5) are created when a load (6) is placed on the TAD during operation. Because

of these moments, which need to be supported by the shaft, the opposing heads, and the deck, the machine must be more robust, and therefore more costly. Additional stresses are caused due to the expansion of components during the heating process to arrive at steady-state operation. Because of these difficulties, some research has gone into producing a more optimum through air drying apparatus. (A full TAD assembly can be found in Figure 2.2.)

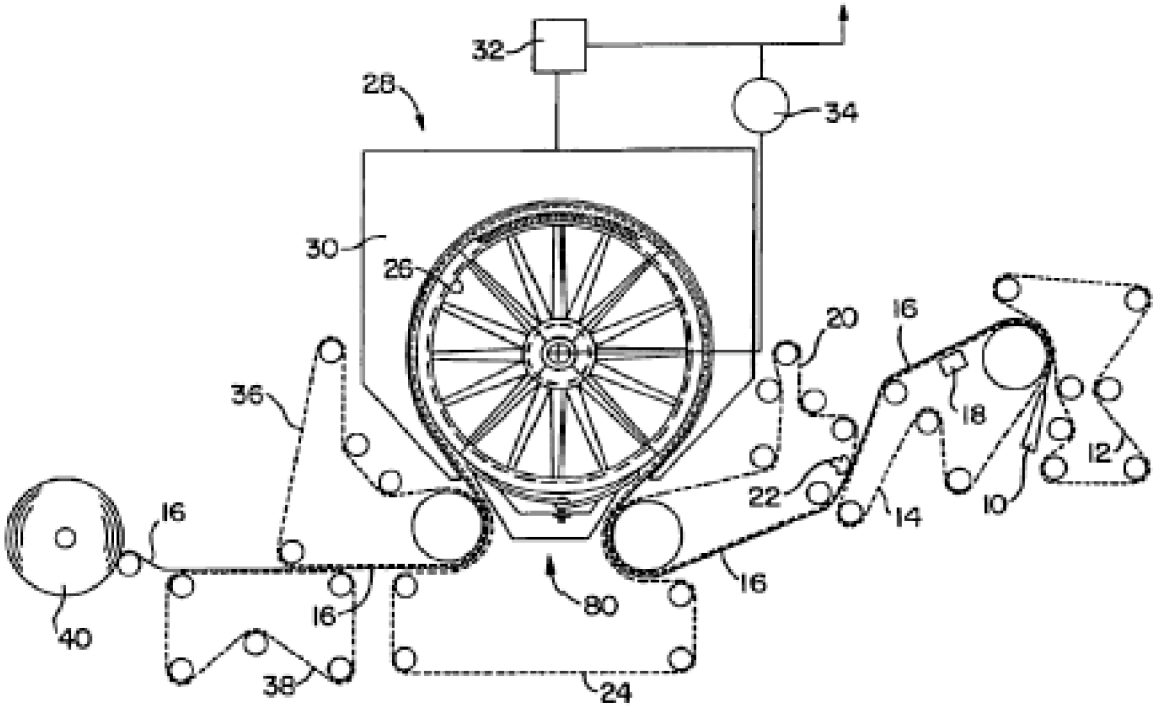

Figure 2.2 - TAD Assembly[2]

2.2.2 Reduction of Pinholes

Pinholes are tiny holes in the paper that are an undesirable effect caused by a variety of reasons. As discussed above, one of the sections of the TAD process is deflection of the papermaking fibers into the deflection conduits in the TAD fabric. A preferred method

of accomplishing this deflection is by exposing the web to a vacuum through the deflection conduits. As a result of this pressure differential caused by the vacuum, the web deflects into the network surface. However, quite often, some of the deflected fibers will separate from the web and pass through the papermaking belt. This causes the formation of pinholes in the paper sheet and often causes clogging in the vacuum machinery.

Because pinholes are such an undesirable characteristic in both the quality and the aesthetics of the finished paper sample, a great deal of research has gone into adapting the TAD process to reduce the pinholing in the finished paper sheet. One example of a way to accomplish this comes from an invention by The Procter & Gamble Company[4].

In this invention, after the papermaking web is molded on the forming wire, it is transferred to an air permeable belt – one side of which contacts the web. Next, the web is overlaid with a flexible sheet of material having a sheet air permeability that is less than the permeability of the belt[4]. This can be seen in Figure 2.3 where the paper web is sandwiched between the belt (20) and the flexible material (30).

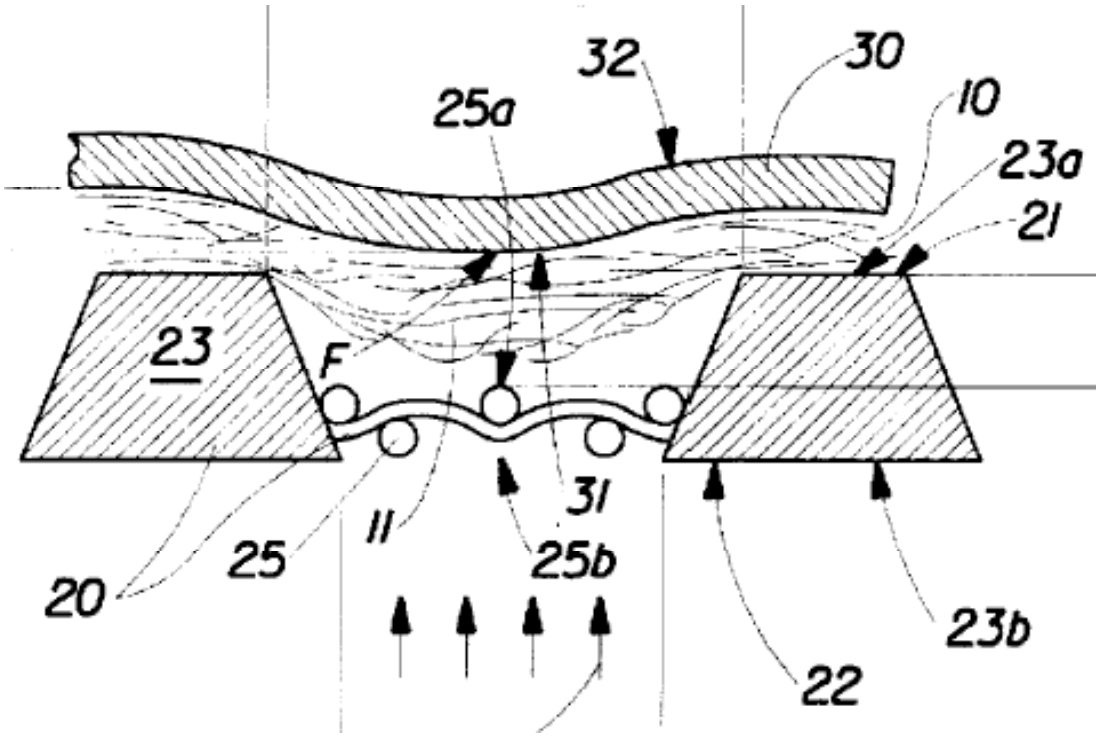

Figure 2.3 – Paper Web between Belt and Flexible Material to Reduce Pinholing[4]

Preferably the flexible sheet has an air permeability that is very low, and ideally, it is completely air impermeable, whereas the belt has a very high level of air permeability. Then when the vacuum pressure is applied, it pulls the paper web and the flexible sheet into the deflection conduit. This can be seen in Figure 2.4. Since the web is in direct contact with the sheet, the paper fibers are not subjected (or at least not subjected as much) to the direct action of the vacuum pressure. This both reduces pinholing in the final sheets and also creates a more uniform basis weight throughout the sheet.

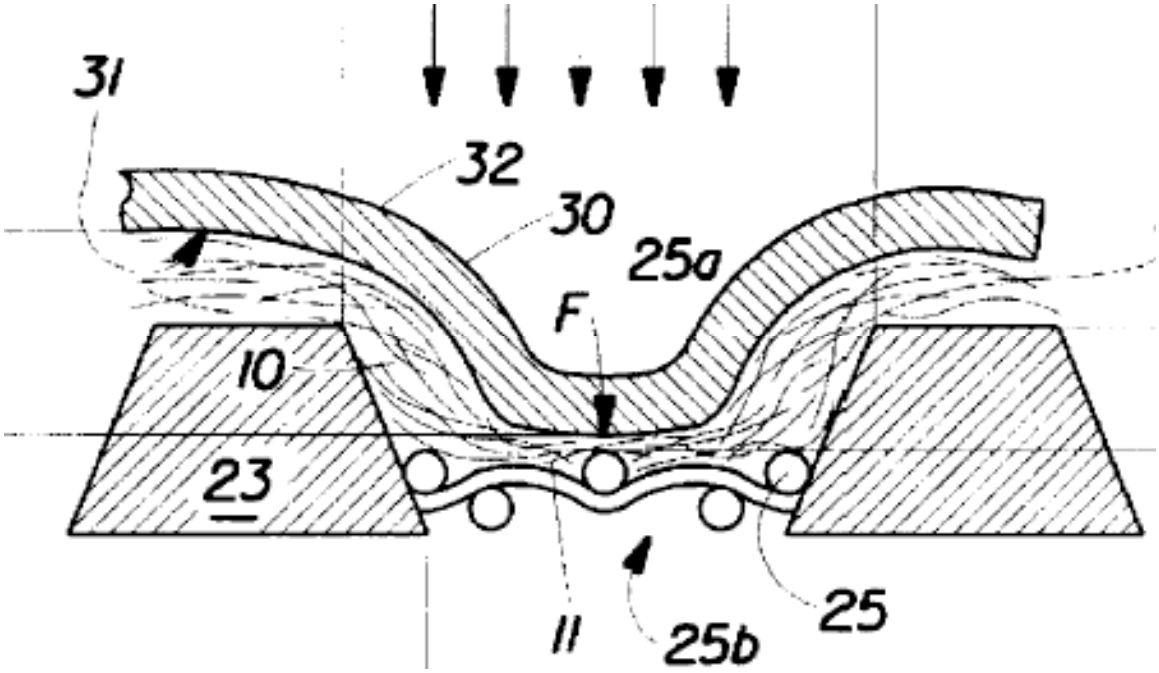

Figure 2.4 – Deflection of Paper Web between Belt and Material[4]

2.2.3 Increased Quality of Molding a Paper Web

Another way of forming molded paper sheets is by using a press nip to increase the deformation of the paper web into an imprinting fabric. As discussed in Procter & Gamble's patent 5,893,965, a compression nip which presses the moist paper web between an imprinting fabric and a press felt can cause enhanced deformation of the paper web. Some studies have investigated the effect of the final paper geometry and physical properties with regard to the geometry of the press nip[4].

One way to improve upon these methods of shaping sheets is by adding shear. Shearing the web as it is being compressed creates a variety of benefits including better molding, enhanced mechanical and absorbency properties, and otherwise unachievable textures or geometries[5]. Another improvement, which can add to the improvement of shearing, is

the use of new deflection members such as those shown in Figure 2.5 which can create asymmetrical protrusions in the paper web.

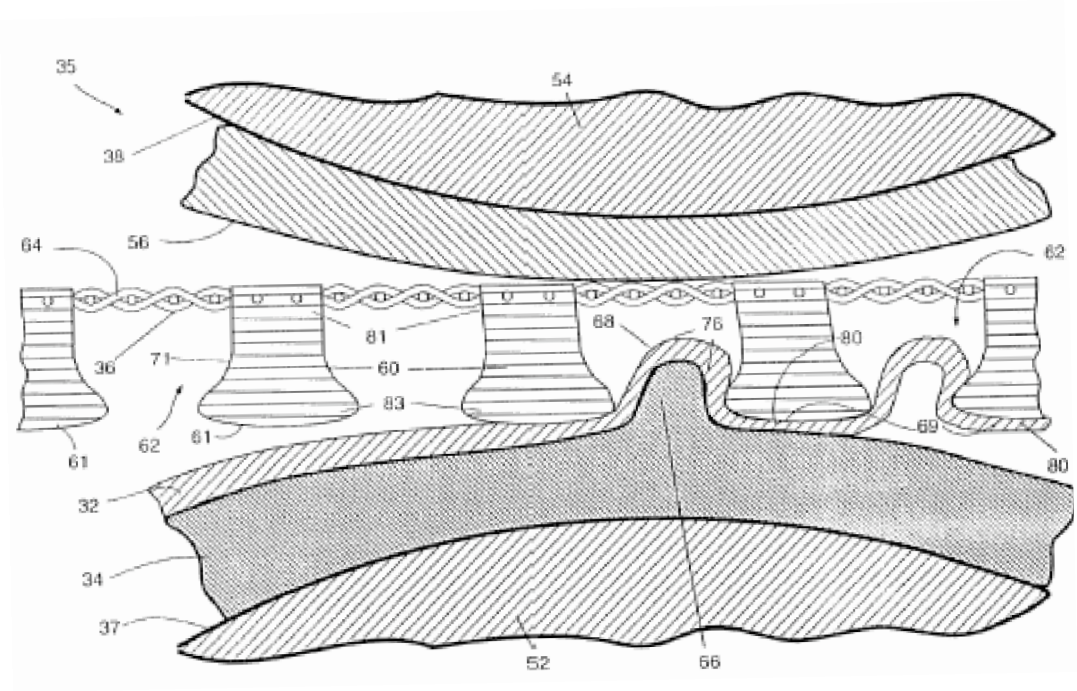

Figure 2.5 – Asymmetrical Deflection Members[5]

This interesting asymmetrical geometry can have potential advantages. These advantages are especially apparent in unique tactile properties. Depending on the actual geometry of the members, the paper bump, or dome, may be more flexible and can have bi-directional frictional properties. This could give a paper a soft feel in one direction but a higher friction in the opposite direction that would be better for scrubbing.

2.3 Shaping Fabrics

The shaping fabric is a crucial part to the geometry and quality of the final paper sample, and much research has gone into this topic. Often the research is to aid the process and improve the final quality of the paper sample. However, a great deal of interest lies in the

ability of the foraminous member to aid the aesthetic aspect of the sample by creating varied geometries and shapes in the paper.

Most foraminous members are comprised of two regions – the network surface and the openings for the deflection conduits. These can be seen in Figure 2.6 where the network surface is shown as 23 and the deflection conduits are 29.

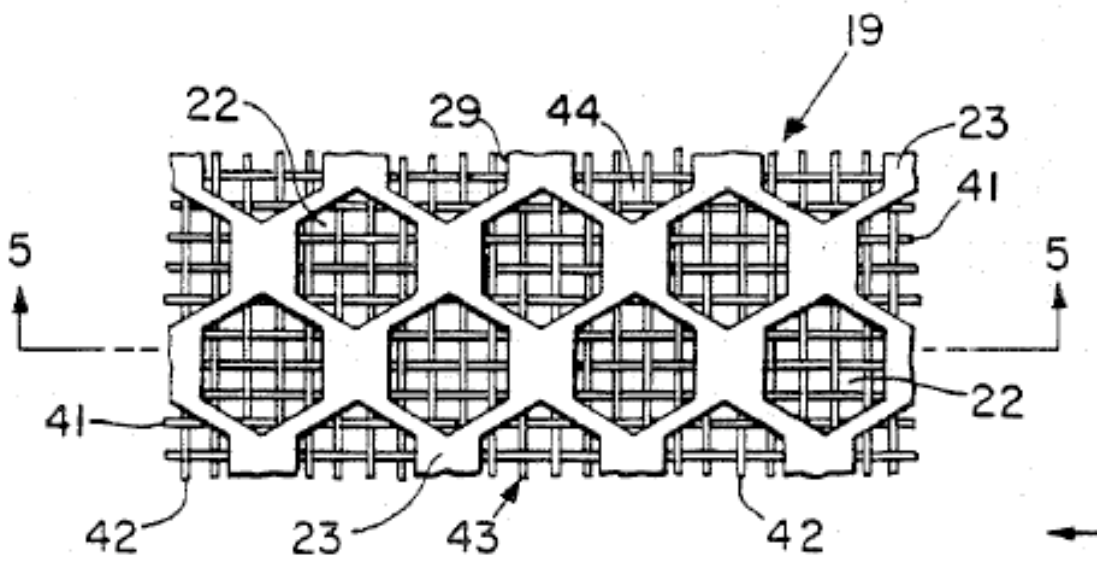

Figure 2.6 – Composition of Foraminous Member[6]

Selection of the parameters defining one region will inevitably affect the parameters of the other region. While the openings of the deflection conduit can be random in shape distribution, it is not the preferred manner. As mentioned in the United States Patent 4,528,239 of Paul Trokhan, "an infinite variety of geometries for the network surface and the openings of the deflection conduits are possible.[6]" However, he has set certain broad guidelines for defining them.

One guideline is that regularly shaped and organized geometries produce a more regulated final sheet, especially with regard to its physical properties. Another is that the open area of the deflection member should be somewhere between 35-85% of the total surface area. Also, to increase the paper strength, it is certainly desirable to reduce localized stresses. To achieve this, the ratio of the diameter of an inscribed circle in the geometry of the opening (d) to the shortest distance of centers to the next opening (b) should be between 0.45 and 0.95 (See Figure 2.7.)

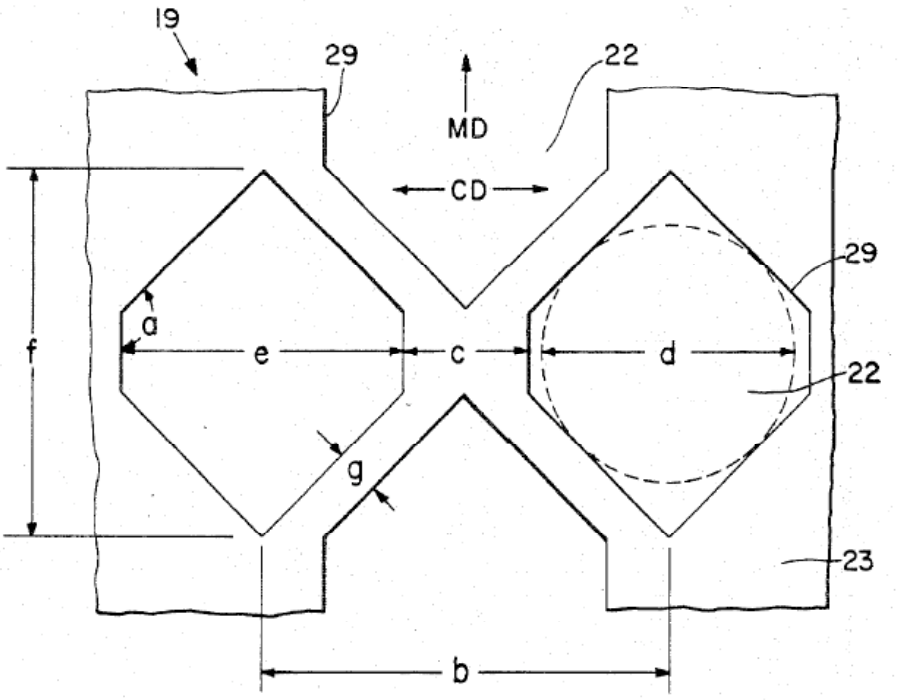

Figure 2.7 – Ratio of Open Area to Closed Area[6]

Certainly the previous model is fairly simple. Further research has gone into developing foraminous members that can create more complicated geometries without compromising the physical qualities of the paper sheets. A way to accomplish this is with a member that has at least two background regions separated by a visually distinctive transition region.

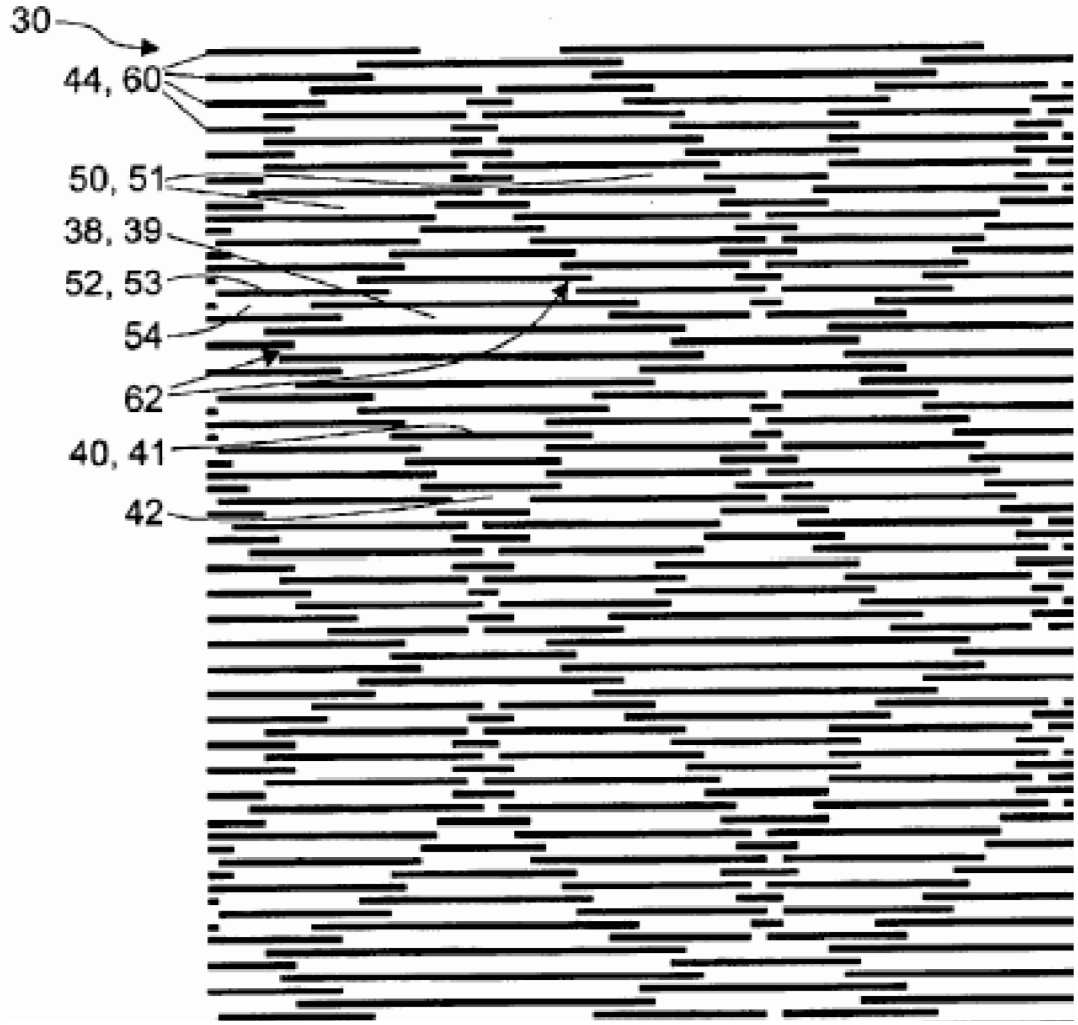

Figure 2.8 – Continuous Transition Regions[7]

The transition regions can be seen in 62 in Figure 2.8. The transition region separates the first and second background regions, defines the decorative shapes, and can comprise curvilinear shapes. The transition region can form a visually distinctive pattern by a variety of methods. The transition region could have a depth deeper than the background regions or a depth somewhere between the depths of the background regions[7]. These transition regions, produced by knuckles in the fabric, can be arranged in a complex pattern, such as butterflies or fish, as can be seen in Figure 2.9. This is advantageous for

a few reasons. One is obviously just the marketability of more aesthetic designs. However, company branding and other opportunities can arise.

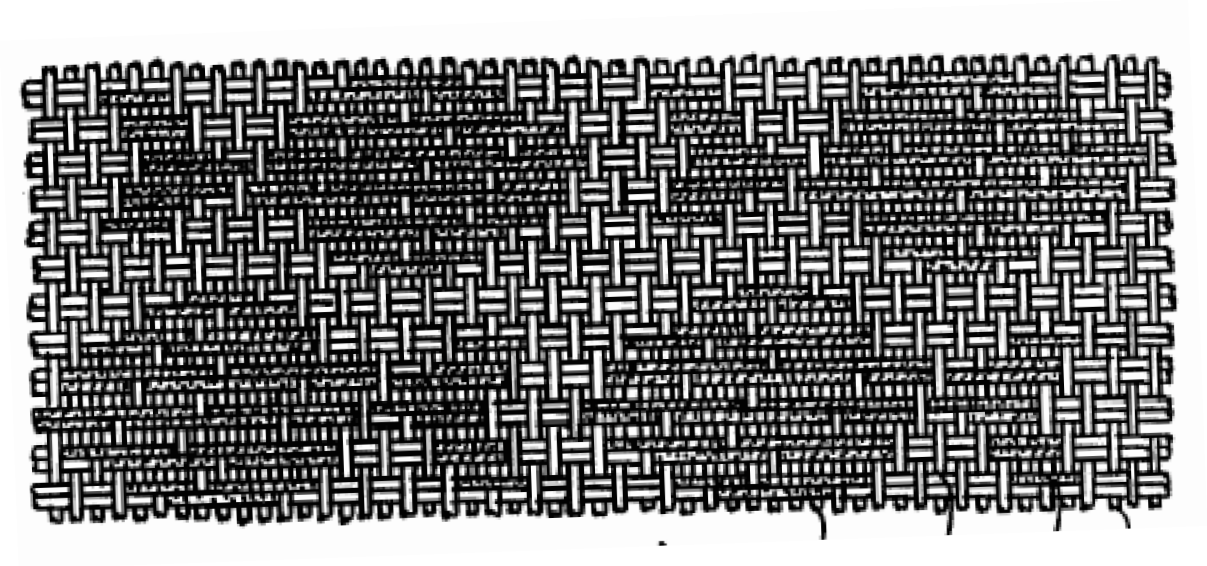

Figure 2.9 – Fish design in Foraminous Member[8]

Members such as these can be created in a few different ways. One option is woven fabrics, as can be seen in Figure 2.10. With woven fabrics, there are yarns in the fabric traveling in the machine direction, called warp yarns and yarns in the cross-machine direction called shute yarns[8]. These yarns can be round, flat, or ribbon-like, or any combination thereof. These choices allow for a wide variety of geometries.

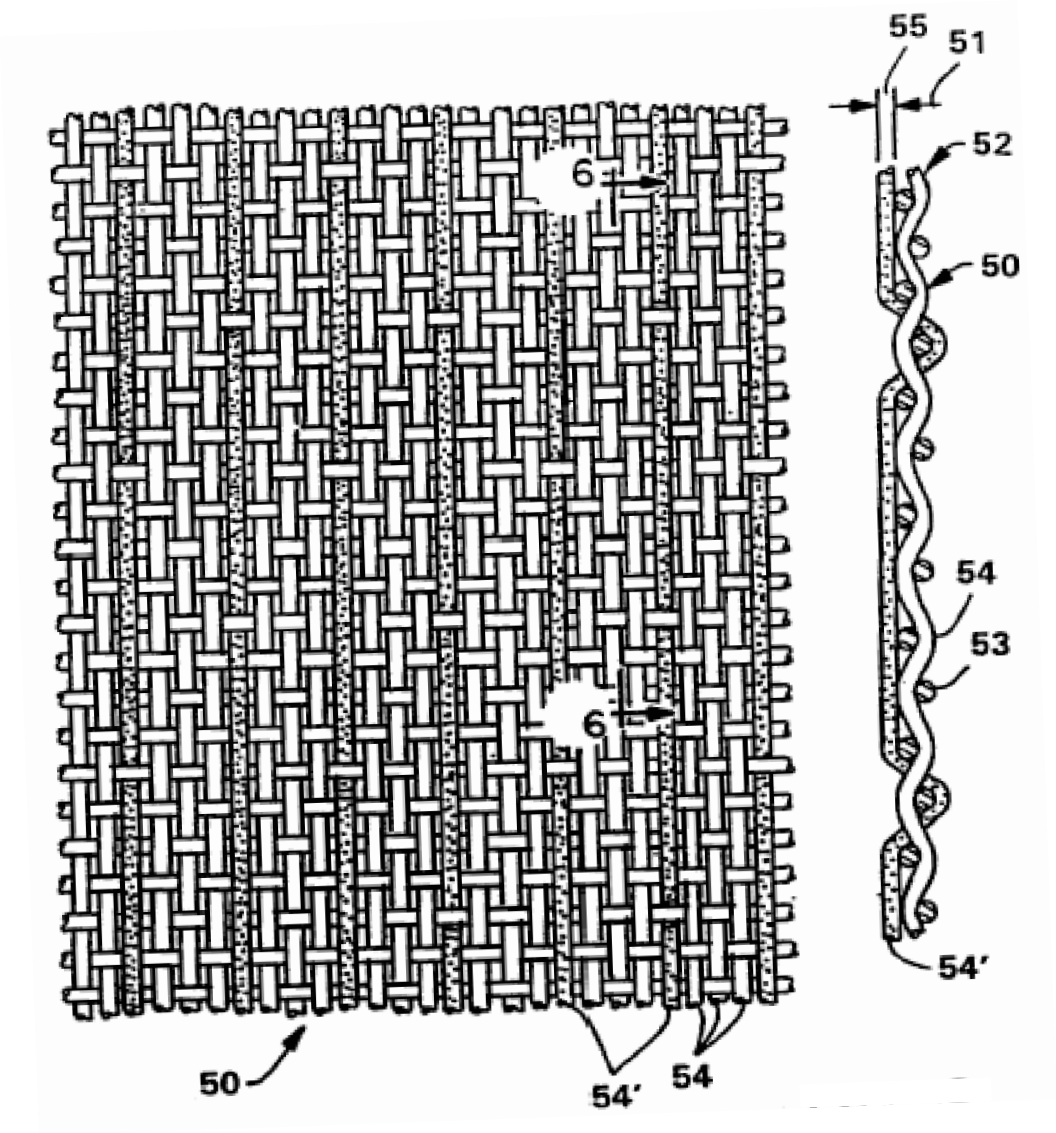

Figure 2.10 – Woven Fabric[8]

Another possibility for these foraminous members is a composite sculpted fabric. An example of this possibility is shown in Figure 2.11. This fabric is composed of a base fabric with raised elements. The base fabric can be a woven or nonwoven fabric having the raised elements being formed by some method of photocuring the elevated resinous elements. While the example in the figure is relatively simple, various other topological

elements can be part of the surface as long as there is a possibility of creating a visually distinctive molded paper web.

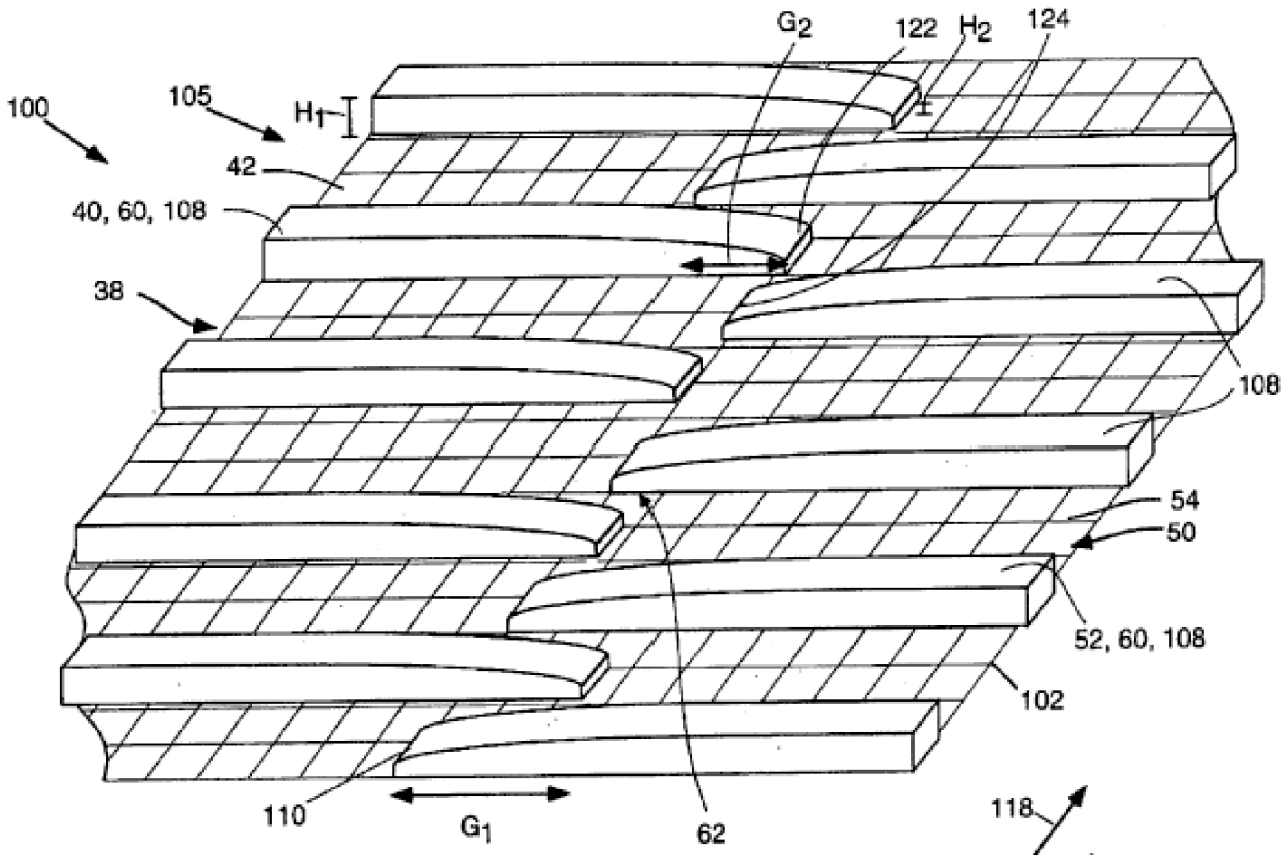

Figure 2.11 – Composite Sculpted Foraminous Member[7]

As can be seen through this literature review, comprised almost exclusively of patents, most of the information about these types of products is tied up in companies. This is because even small differences can set one company's product apart from that of another.

It can also be noted that a great deal of research has gone into this area – especially in the development of the foraminous members. These are important in increasing the

aesthetics of the final product and making it more marketable. However, very little research has been done on the limitations of these products and processes in a quantitative way. Paul Trokhan revealed only limited data about this[6], but it is important information to consider. Especially with the newer processes of making foraminous members, such as the composite structures shown in Figure 2.11, more complicated geometries can be achieved, however, it is important to know their limitations.

3 EXPERIMENTAL SETUP AND PROCEDURES

This research investigates the effects of three different types of parameters on thickness: mold geometry, process, and paper. The experimental research is fundamental in nature. The molding structures are of a simplified geometry that is produced via rapid prototyping techniques rather than the commercially used molding fabrics. Also, the testing is completed using a simplified laboratory simulation of the process rather than on a full-scale machine.

3.1 Creation of Molds

The first part of this experimental process involved creation of the molds on which to form the paper samples. These molds were created using rapid prototyping technology, which allows fast, cost-effective way production of single parts. These parts can have very complex geometries that cannot be produced using traditional manufacturing processes.

To begin, a three-dimensional design for the mold was created using Pro/Engineer software. Examples of the CAD model can be seen in Figure 3.1 and 3.2. The file is then saved in a specific file format that will allow it to be read by the rapid prototyping machine.

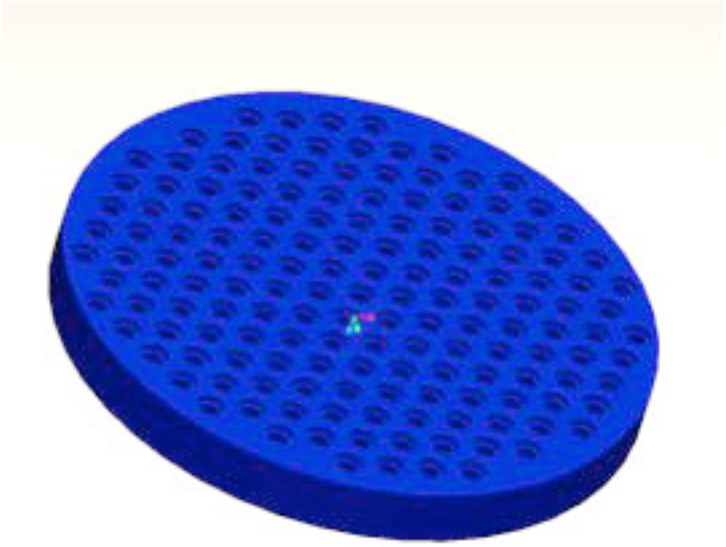

Figure 3.1 – Pro/Engineer Model of Mold

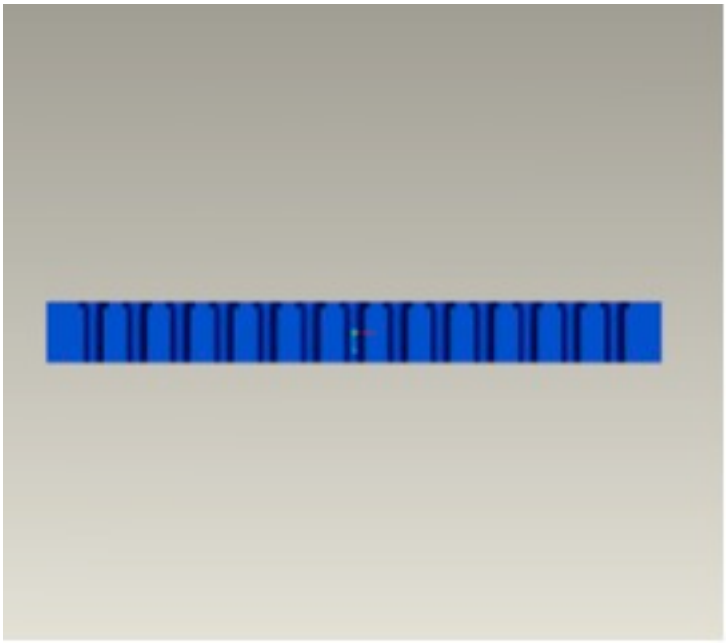

Figure 3.2 – Pro/Engineer Model of Mold (Cut-away)

The rapid prototyping technology used to produce the molds for these experiments was Stereolithography (SLA). In this process, a laser makes two-dimensional scans on the top surface of a vat of liquid photopolymer resin. In all areas that the laser touches, a chemical reaction occurs, causing the resin to solidify[9]. A picture of an SLA machine can be found in Figure 3.3.

Figure 3.3 – Stereolithography Machine

The CAD file is first split into many small cross-sections. Support structures are built on the build platform. (See Figure 3.4 for schematic.) These allow the part to be removed from the platform without damaging the actual part. After the support structures have

been generated, the laser traces the first cross-section. The platform lowers slightly into the resin vat and the next cross-section is traced. This process continues until the part is built. Then the part is pulled from the build platform and all support structures are removed. It is then rinsed in isopropyl alcohol, which works as a solvent to remove any uncured resin from the part. Finally, the part is post-cured by means of UV exposure to fully develop the photopolymer resin. A photograph of one of the molds used in the experiments can be seen in Figure 3.5.

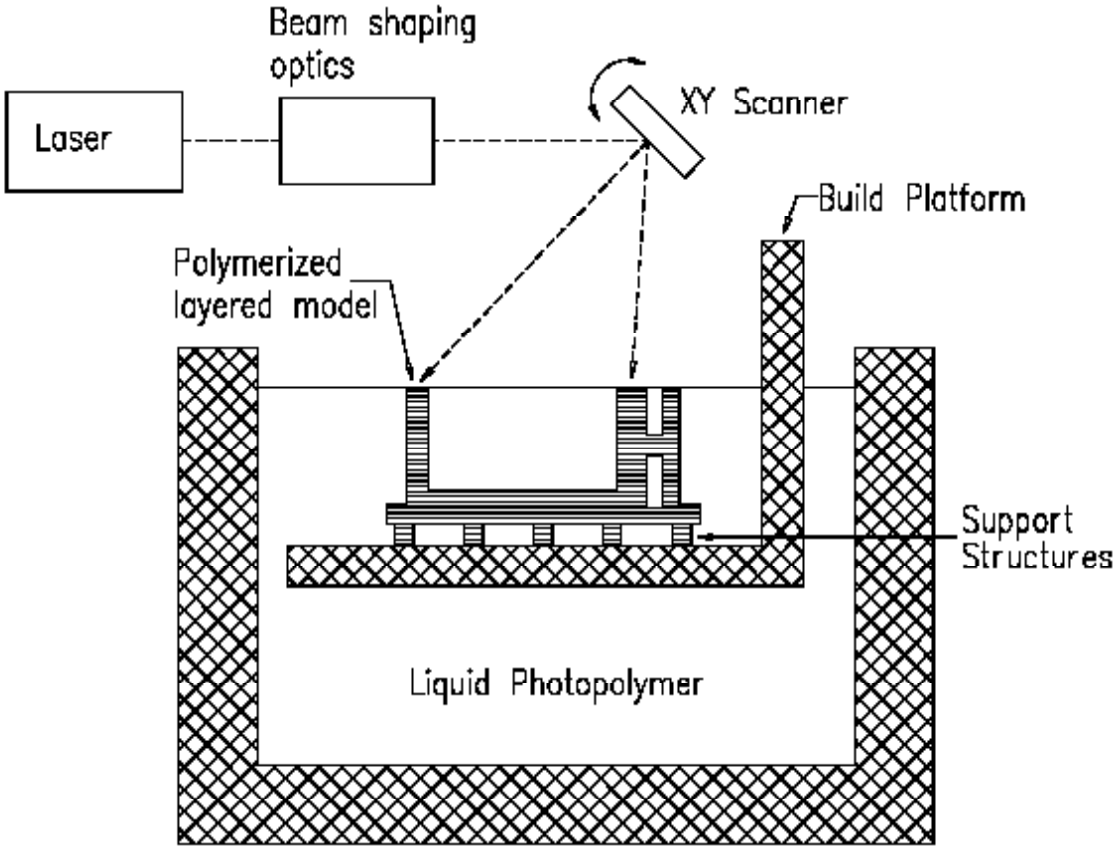

Figure 3.4 – Stereolithography Schematic

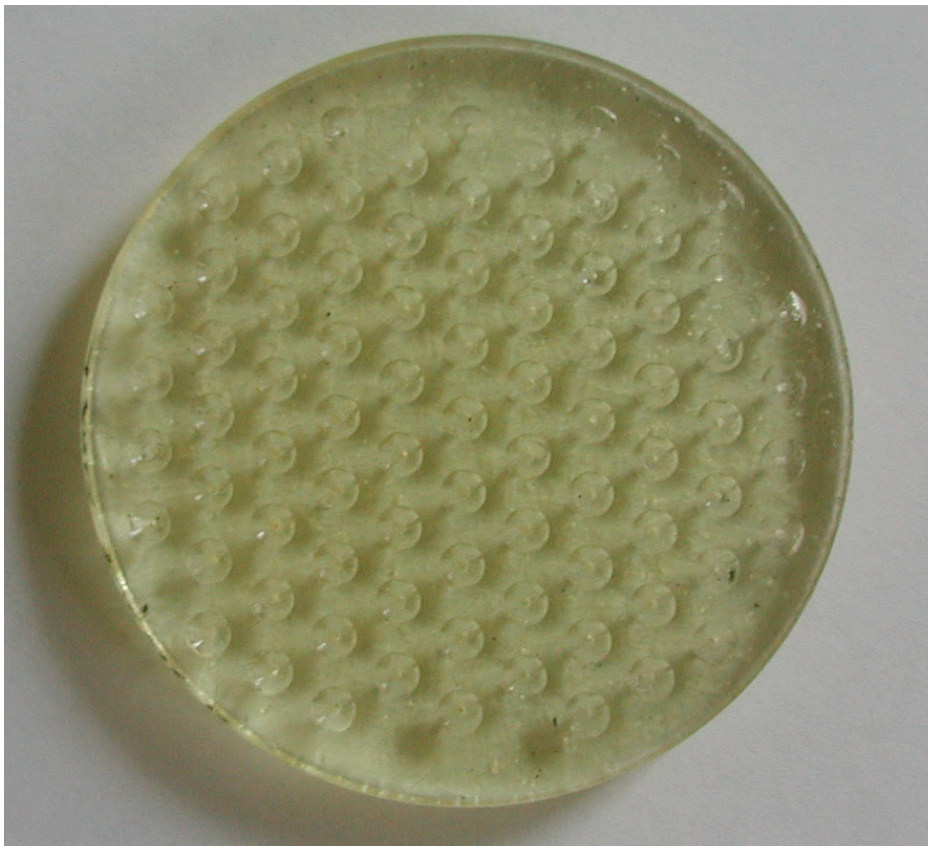

Figure 3.5 – Stereolithography Mold

3.2 Creation of Paper Samples

3.2.1 Refining

The pulp used for paper samples was refined in a Standard Valley Beater. The target freeness was ~650 CSF. About 450 grams (+/- 5%) of International Paper Bleached (Softwood) pulp was torn into pieces and placed in the Valley Beater (Figure 3.6). Twenty-three liters of deionized water was added, and then the machine was turned on allowing the pulp to circulate with no load for a few minutes[10]. An initial freeness reading was obtained.

Figure 3.6 – Valley Beater

The beater weight was then placed on the bedplate lever arm, and the refining operation initiated. Samples were taken from the pulp slurry at regular time increments and the freeness was measured. (Time increments were adjusted based on the previous freeness measured.) When the pulp reached the target freeness, refining was stopped.

To complete the freeness test, filter papers were heat dried to remove all moisture and weighed. Three hundred mL of pulp was taken from the valley beater, and water was added to yield a total volume of 2L. The diluted pulp slurry was disintegrated for 50,000 revolutions. After disintegration, the freeness of the pulp was measured[11].

3.2.2 Creation of Test Sheets

Using the refined pulp stock, approximately 25 g of pulp are mixed with 2.5 g of standard grade Kymene 557H (12.5% solution). This is mixed with approximately five gallons of water until it is a homogenous mixture. A full test sheet must be made to calculate the exact amount of pulp to create a sheet of the proper basis weight. Using a set volume of pulp, the test sheet is made. It is then fully dried to remove all moisture and weighed. To achieve the target basis weight, this test sheet should weigh 0.6 grams. A simple calculation can calculate the volume of pulp needed:

$$\frac{0.6g}{\text{Vol. needed (x)}} = \frac{\text{Weight of Test Sheet}}{\text{Volume Used}}$$

This equation is solved for x and that is the volume of pulp to be used for the test sheets.

The test sheets that are needed for the experiments are 2.5 inches in diameter. The test sheets are created on forming fabrics, which must be completely saturated before use. First the hand sheet mold is flooded. As this occurs, the forming fabrics are slid onto the sheet mold forming wire, avoiding any air bubbles. The forming fabrics are then secured with a metal ring. Once all three forming fabrics are secured on the forming wire, the mold cylinder is closed. As the water is filling the cylinder, the set volume of pulp is added. Once the mold cylinder is filled, the water flow is stopped. After mixing the solution a few times with the perforated stirrer, the water is drained. The test sheets are then carefully removed and placed into a sealed container to avoid drying.

3.3 Shaping of Paper Samples

The paper sheets were formed using a Vacuum Test Head machine (VTH). The VTH, which is shown in Figure 3.7, is a test device that is used to simulate the vacuum dewatering and shaping process on a paper machine. The VTH is composed of four main parts. First there is the test head that holds the mold and therefore the paper sample. There are two vacuum tanks (not shown in Figure) that provide the vacuum pressure. There are also two computer-controlled air activated ball valves that control the amount of time the test sample is exposed the vacuum source. Finally, there are the computer controls and data acquisition (not shown in Figure) to run the experiment and obtain the results[12].

A computer program controls the VTH; it activates the solenoid air actuators that activate the ball valves. The ball valves control the amount of time that the sample is exposed to vacuum. (The minimum obtainable dwell time is 25 milliseconds.) The valves are plumbed in series and connect the test sample to the vacuum source. Prior to the test, the valve that is closest to the test sample (top valve) is normally closed and valve closest to the vacuum tank (bottom valve) is normally open (see Figure 3.7). The test is initiated by opening the upper valve, exposing the test sample to a vacuum source. The test ends by closing the lower valve.

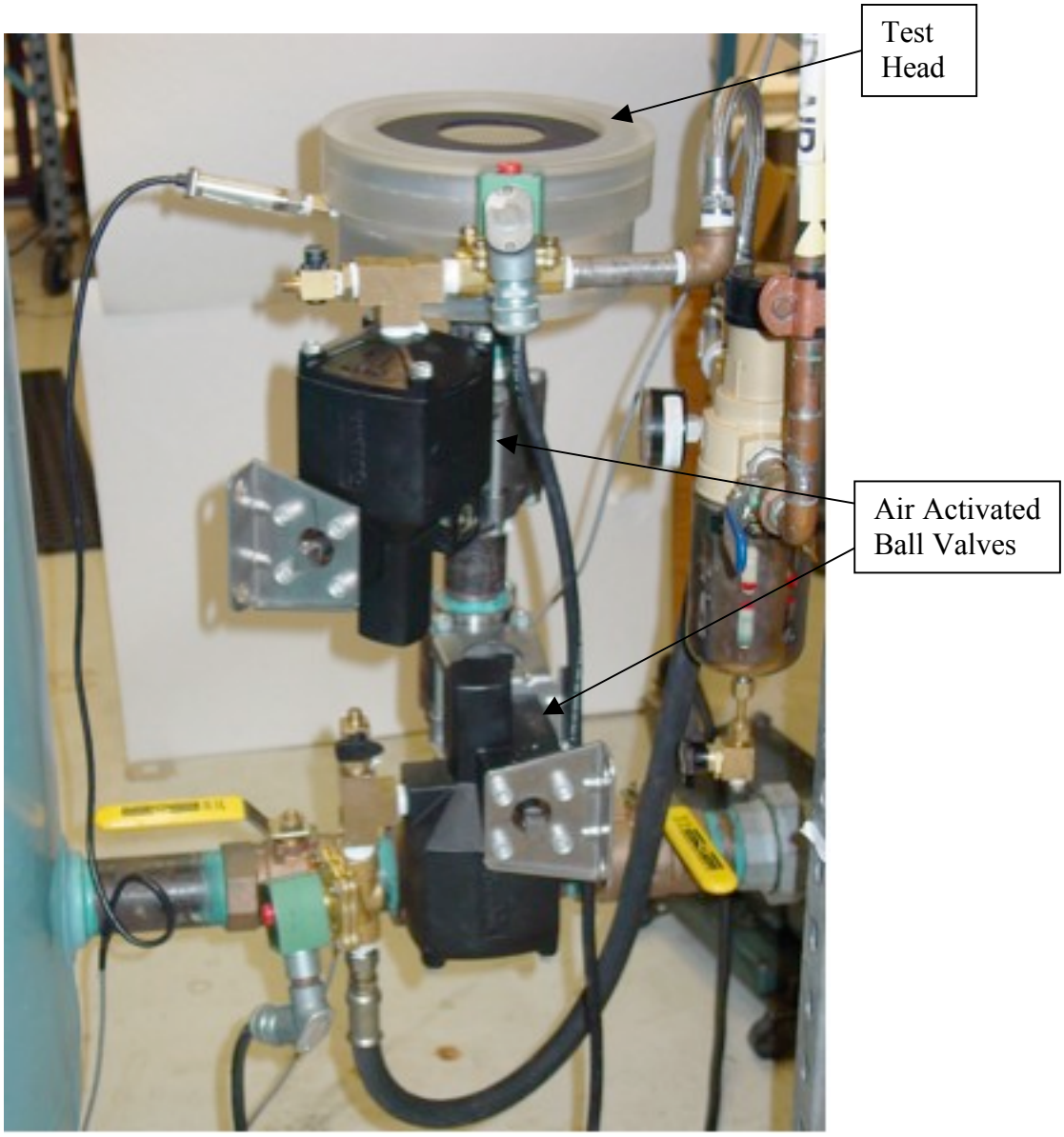

Figure 3.7 – VTH Setup

The test head can be seen more clearly in Figure 3.8. The base of the test head is a drilled plate. This supports a TAD fabric on which the mold is placed. The mold is 2.5 inches in diameter and is surrounded by a gasket. The gasket and TAD fabric are supported by an acrylic cover that encloses the test head and prevents edge leakage. The paper sample (still on the forming fabric) is positioned face-down directly on top of the mold.

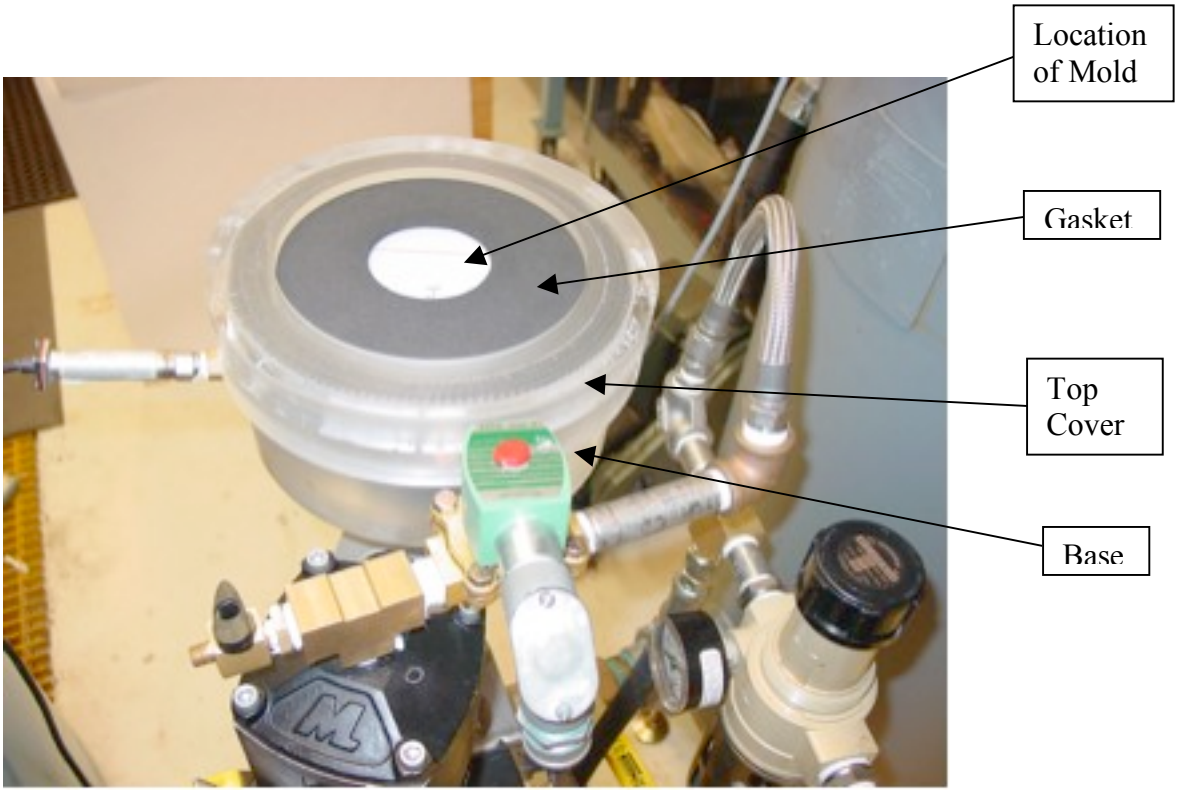

Figure 3.8 – VTH Test Head

After setting the vacuum level to the desired amount, the valves are set to their start position. Prior to testing, the recently made samples are stored in an airtight container. Immediately before the test, the sample is transferred to the mold. The test is then initiated. The vacuum pulls the paper sample down into the geometry of the mold creating a shaped test sheet. After the test, the paper sample is carefully removed and placed in an oven to completely dry. The VTH is then reset for the next run. A photograph of one of the molded paper samples can be seen in Figure 3.9.

Figure 3.9 – Molded Paper Sample

3.4 Thickness Analysis

There were many challenges developing a simple, reliable, and repeatable method for determining the thickness of the test sheets. First, a caliper measuring technique was tried. In this technique, the paper samples were stacked and placed under a thin

plexiglass sheet to reduce the pressure applied at any one point in the sample. The caliper measurement was used without any additional weight added, as the sheets are delicate. However, the results using this technique were inconsistent. Simply by examining the sheets, it was clear that the sheets with the larger domes were thicker than the sheets with the smaller domes. However, using this test, the results did not support this visually observed characteristic. There are likely two reasons for this. The first reason is that the paper samples were nesting, i.e., when measuring a series of samples, the domes were nesting and therefore giving an inaccurate, thinner thickness. A second reason is that the samples were too fragile, and even without the additional weight, the caliper gauge is applying approximately 50 grams of mass – more than the sheets could withstand without significant compression[13].

Next, a shadow moiré technique was used[14]. This technique is capable of characterizing and analyzing surface contours not just quantitatively but also visually. This is accomplished by using a camera to capture the surface contour of the sample as the platform holding the sample moves vertically through a controlled sequence. A computer analyzes the observed fringe pattern changes during this sequence and generates both a topography and a maximum and minimum value of the sample height[15]. After many attempts to utilize this technique effectively, it was found to be unsuccessful for the samples for two reasons. First, the paper samples were somewhat curled. After successfully addressing this problem, it was realized that the curling was not the only problem. The sample size was too small for the particular equipment used in the application of the shadow moiré technique.

This led to a final technique. This technique is less sophisticated than the other two, however, it addresses the problems encountered in the caliper testing and produces accurate results. First, some preparatory steps were taken to ready the samples for measurement. To address the fragility of the samples, each sample was sprayed with a light coating of Aquanet hairspray, which acted as a fixative. This makes the samples more robust without affecting the thickness. Each sample was then glued, using a glue stick, to a sheet of medium weight paper to prevent the samples from nesting when stacked.

After the samples were prepared, they were stacked between two plexiglass sheets and measured using calipers (See Figure 3.10.) To ensure maximum consistency, the calipers were slowly closed just until the pressure was enough that they could no longer freely slide over the plexiglass. The thicknesses of the sheets and the mounting paper were also measured using calipers, and these values were subtracted from the total thickness. This value was then divided by the number of samples to find the average thickness of one sample.

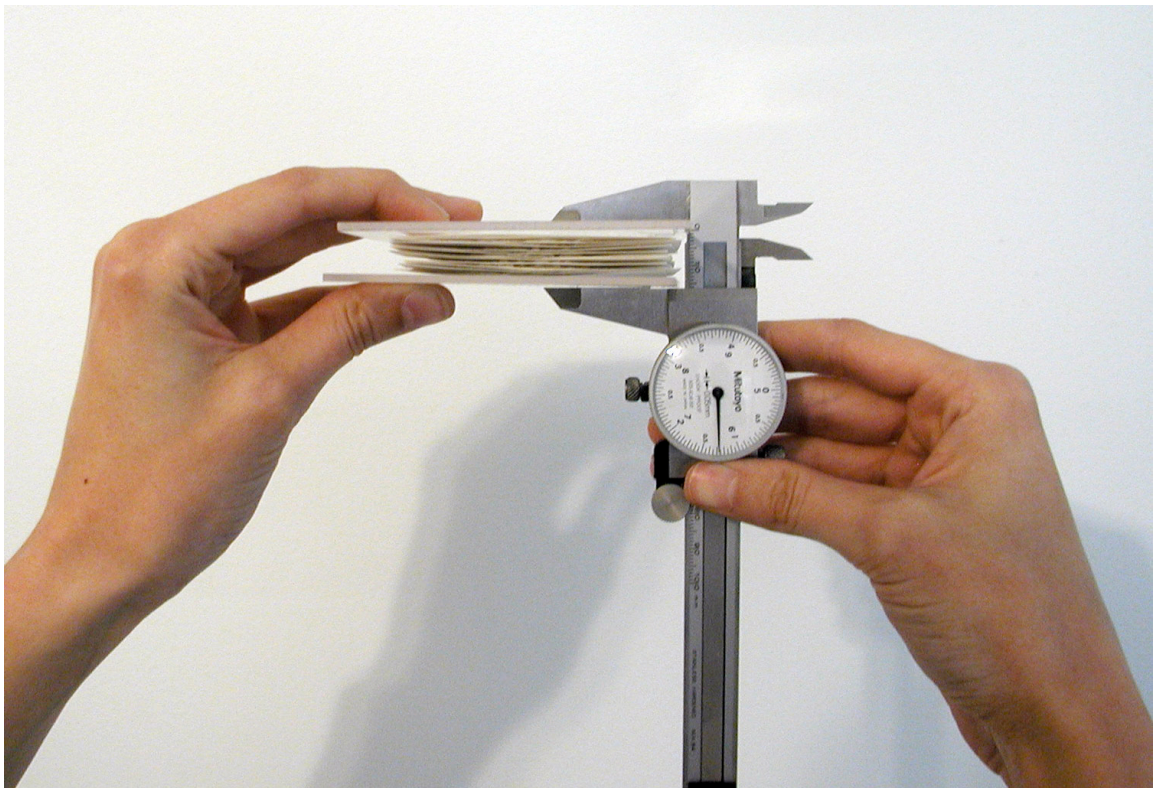

Figure 3.10 – Thickness Measurement

4 MATHEMATICAL MODEL

The mathematical model is based upon an analysis of a linearly elastic, axisymmetrically loaded circular plate in *Advanced Strength and Applied Elasticity*[16]. Utilization of this model is based on the assumption that there is an isotropic, homogenous circular plate with a symmetrical applied load. This model considers the radial and tangential moments as well as the vertical shear force to calculate the maximum deflection at the center of the plate. The model is presented in this chapter but is discussed in relation to the experimental data presented in the next chapter.

The deflection w, of a circular plate will depend only upon radial position if the plate is loaded axisymmetrically, that is, the applied load is symmetrical around an axis through the center of the plate. Therefore, only the radial and tangential moments, M_r and M_θ, and the vertical shear force, Q_r, act upon this circular plate. This can be seen in Figure 4.1.

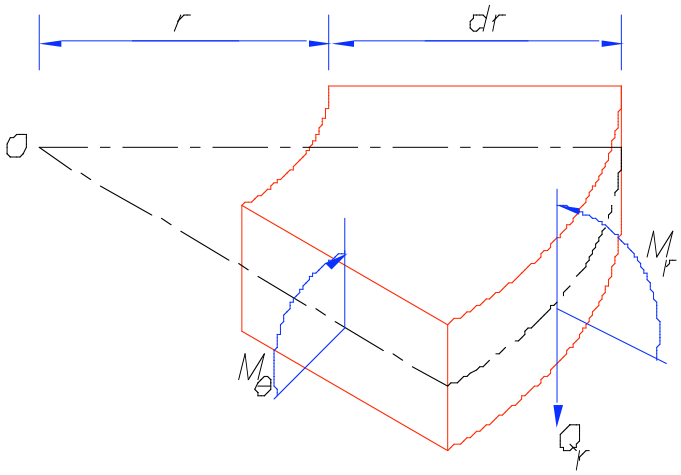

Figure 4.1 – Cutaway Free-Body Diagram

For the axisymmetrically loaded circular plate, these moments and forces can be found from:

$$M_r = -D\left(\frac{d^2w}{dr^2} + \frac{v}{r}\frac{dw}{dr}\right) \quad \text{Equation 4.1}$$

$$M_\theta = -D\left(\frac{1}{r}\frac{dw}{dr} + v\frac{d^2w}{dr^2}\right) \quad \text{Equation 4.2}$$

$$Q_r = -D\frac{d}{dr}\left(\frac{d^2w}{dr^2} + \frac{1}{r}\frac{dw}{dr}\right) \quad \text{Equation 4.3}$$

Where,

r is the radial position

ν is the Poisson's ratio

D is the flexural rigidity (which is assumed constant), defined by

$$D = \frac{Et^3}{12\left(1-\nu^2\right)} \quad \text{Equation 4.4}$$

Where,

E is the Modulus of Elasticity

t is the thickness of the sheet

Based upon Equations 4.1-4.3 and utilizing the identity:

$$\frac{d^2w}{dr^2} + \frac{1}{r}\frac{dw}{dr} = \frac{1}{r}\frac{d}{dr}\left(r\frac{dw}{dr}\right) \quad \text{Equation 4.5}$$

the force balance differential equation for the surface deflection is given to be:

$$\nabla^4 w = \frac{1}{r}\frac{d}{dr}\left\{r\frac{d}{dr}\left[\frac{1}{r}\frac{d}{dr}\left(r\frac{dw}{dr}\right)\right]\right\} = \frac{p}{D} \quad \text{Equation 4.6}$$

Where,

p is the pressure load per surface area

With the origin axis located at the center of the plate, the displacement, w, is found by successive integration of Equation 4.6:

$$w = \int \frac{1}{r} \int r \int \frac{1}{r} \int \frac{rp}{D} dr\ dr\ dr\ dr$$

or

$$\frac{D}{p_o} w = \int \frac{1}{r} \int r \int \left[\frac{1}{r} \left(\frac{r^2}{2} + c_1 \right) \right] dr\ dr\ dr$$

or

$$\frac{D}{p_o} w = \frac{r^4}{64} + \frac{c_1 r^2}{4} (\ln r - 1) + \frac{c_2 r^2}{4} + c_3 \ln 4 + c_4 \qquad \text{Equation 4.7}$$

For an axisymmetrically loaded circular plate, there are three variations of the boundary conditions:

(1) *Clamped edge*, described by:

$w = 0$ Equation 4.8a

$$\frac{\partial w}{\partial r} = 0 \qquad \text{Equation 4.8b}$$

(2) *Simply supported edge*, described by:

$w = 0$ Equation 4.9a

$M_r = 0$ Equation 4.9b

(3) *Free edge*, described by:

$M_r = 0$ Equation 4.10a

$Q_r = 0$ Equation 4.10b

Utilization of this mathematical model is based upon four assumptions:

(1) The deflection of the plate is small in comparison with the thickness of the plate.

(2) Straight lines that are initially normal to the area above the hole remain normal to that surface after bending.

(3) No straining, stretching, or contracting occurs due to the bending.

(4) The stress component normal to the midsurface is negligible.

5 EXPERIMENTAL RESULTS AND DISCUSSION

Experiments were designed to test the importance of the selected experimental variables on the thickness of the sheets. To begin with, some constraints were set. Paper samples were made from the same pulp throughout the experiments, and the basis weight of 30 g/m^2 was held constant.

5.1 Mold Geometrical Parameters

The first set of experiments was intended to investigate the influence of mold geometry on the final thickness. Four molds were created with identical (cylindrical) hole shapes, array patterns, and spacing ratios. The array pattern was hexagonal – three holes were spaced in an equilateral pattern. The array (and spacing) can be seen in Figure 5.1, where r = d/2. Each mold, however, had a different hole diameter. These were 1mm, 2mm, 3mm and 4mm. A vacuum pressure of 15 inches Hg was selected for the testing. Flat control sheets were also created for a baseline measurement.

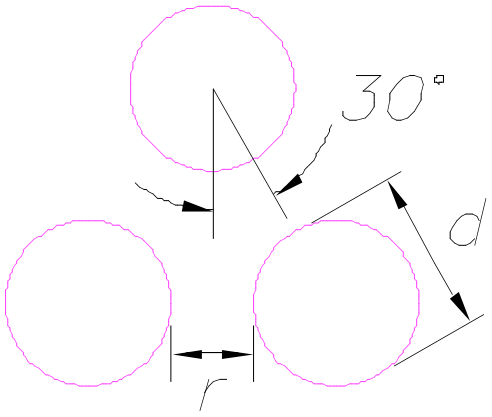

Figure 5.1 – Array and Spacing Pattern of Molds

The hole diameter proved to be a significant factor in the final sheet thickness. The original 4mm diameter mold was abandoned as all sheets formed using this mold had complete breakthrough in the holes. The thickness appears to behave as expected – as the diameter increases, so does the thickness. This can be seen in Figure 5.2.

Following these tests, another series of molds was created. A different geometry was adopted which could potentially accommodate a 4mm diameter. This geometry was a stepped hole. These forms were produced in the following sizes: 2 mm stepping to 1 mm, 3 mm stepping to 2 mm, and 4 mm stepping to 3 mm. A schematic is shown in Figure 5.3. The main concept with the stepped hole is that the stepped hole will help "guide" the paper to form and lessen breakthrough.

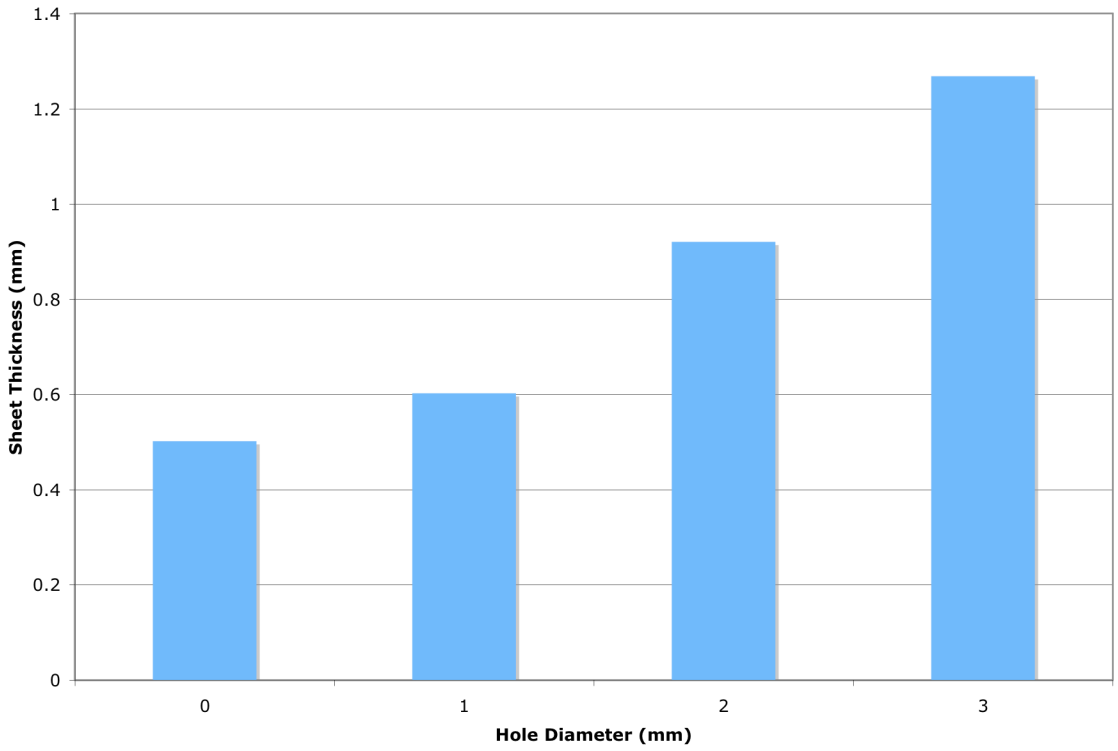

Figure 5.2 – Sheet Thickness vs. Diameter for Linear Circular Holes

The depth (below the top) of the step was based on results from the previous experiment. It was decided that the depth for the larger diameter step (x) should be half the final thickness of the corresponding sheet from the straight hole results. Therefore the depth of the 2mm step was 0.877/2 or 0.44mm. The depth of the 3mm step was 1.314/2 or 0.67mm. And for the 4mm step, it was estimated that the depth was 1.6/2 or 0.8mm.

Figure 5.3 – Cutaway View of Stepped Molds

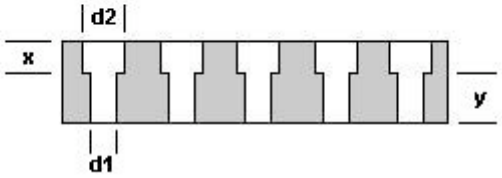

The creation of these molds and test sheets was the same as the previous tests. As the tests began, it was clear that the 4mm step to 3mm was not feasible. These sheets had complete breakthrough for all sheets, and no data is presented. The thickness results for the remaining molds are shown in Figure 5.4. The thickness results compared with the control experiment can be found in Figure 5.5.

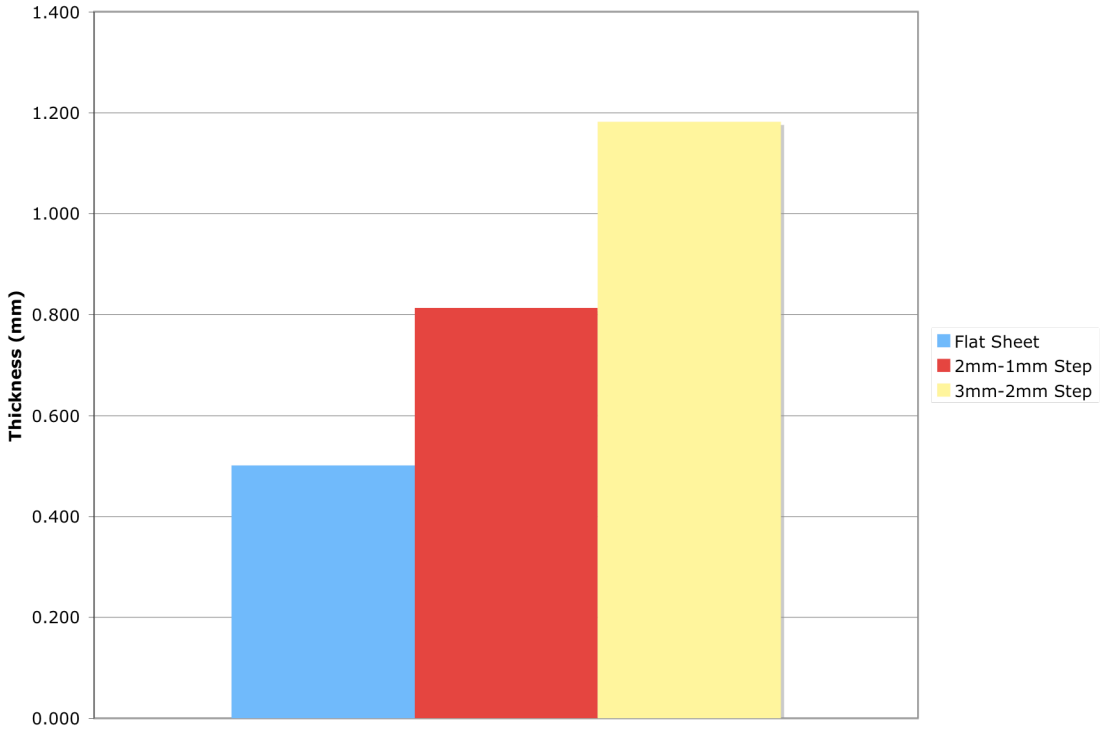

Figure 5.4 – Thicknesses for Stepped Holes

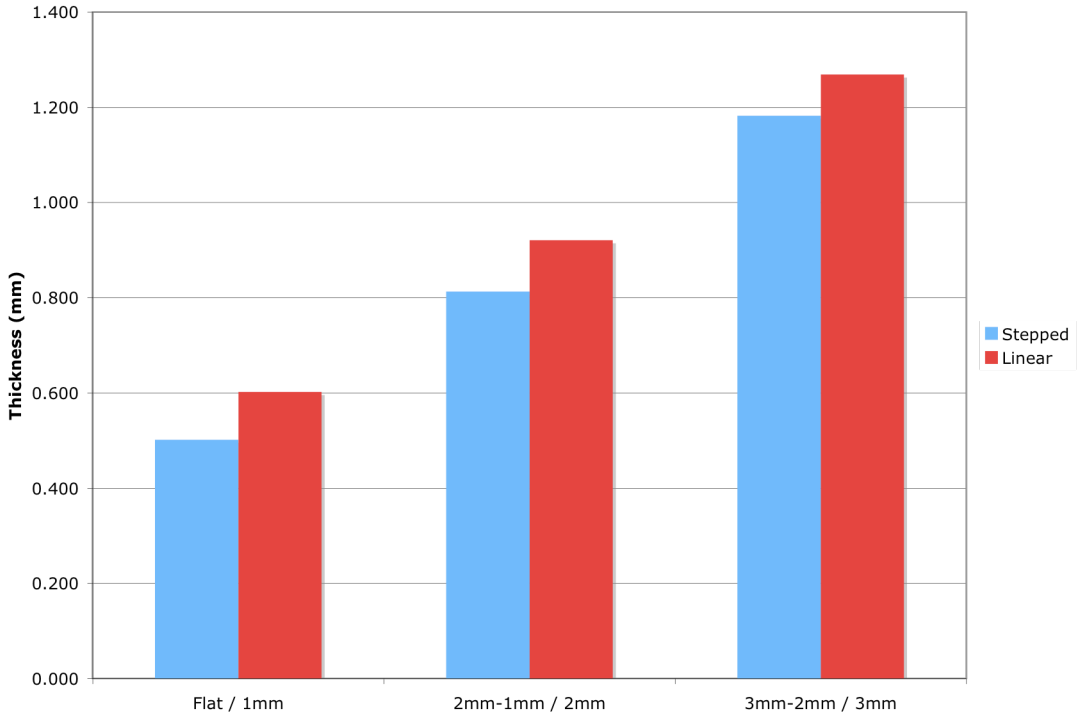

Figure 5.5 – Thicknesses for Stepped Molds vs. Linear Molds

Using the results from these experiments, it is clear that as the hole diameter increases, the thickness also increases. However, this is only to a certain point as can be seen with the experiments with the 4mm hole diameter. So the question was how to create a molded sheet with a 4mm hole diameter that would not break through. The concept considered was to create a conical hole. The rationale for the design of this hole is explained next.

Using the data from the 3mm straight linear holes, the surface area of one of the domes was calculated. The surface area was modeled as a cylinder as seen in Figure 5.6.

$SA = \pi r^2 + 2\pi rh$

where

r = radius, 1.5mm
h = height, 1.314mm

Therefore the surface area for the 3mm linear dome was
$SA = \pi(1.5)^2 + 2\pi(1.5)(1.314) = 19.45mm^2$

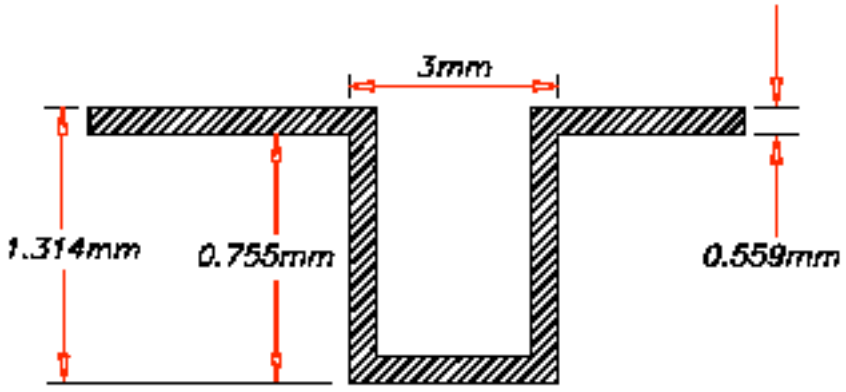

Figure 5.6 – Cylindrical Model

It was then necessary to calculate the height that would give a surface area of 19.45 for a hole that is 4mm at the top. This hole will taper down to a 1mm opening and will be modeled as a cone. The surface area for a cone is:

$$SA = \pi r\left(r + \sqrt{r^2 + h^2}\right)$$

Since this was the equation for the surface area of an entire cone but the paper "cone" being used does not have a base, the surface area to be solved for is actually 19.45 + 3.14(2)2 = 32.01mm^2

$$2\pi\left(2 + \sqrt{4 + h^2}\right) = 32.01$$
$$2 + \sqrt{4 + h^2} = 5.09$$
$$\left(\sqrt{4 + h^2} = 3.09\right)^2$$
$$h = 2.13mm$$

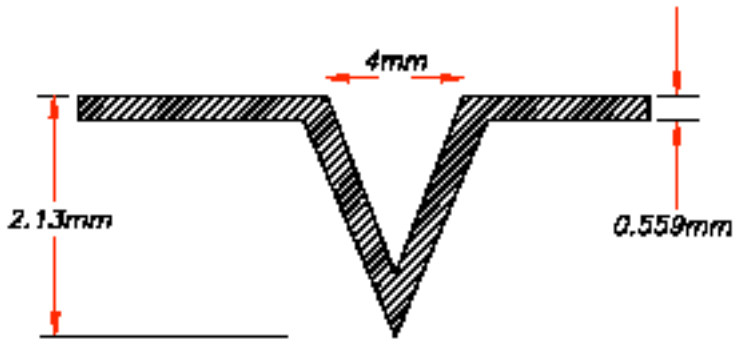

Figure 5.7 – Conical Model

Using the model shown in Figure 5.7, the part was constructed as shown in Figure 5.8. The samples had some pin holes; however, there was no complete break-through as there had been before. Thickness comparison to the control 3mm linear holes can be seen in Figure 5.9.

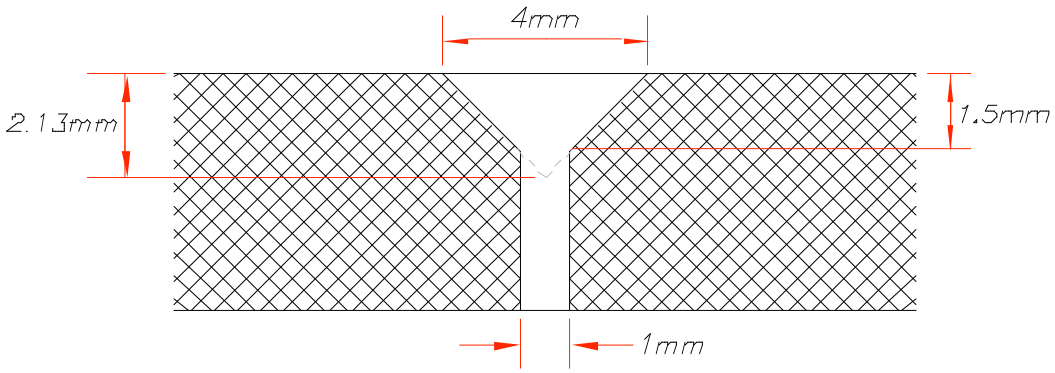

Figure 5.8 – Schematic of Tapered Mold

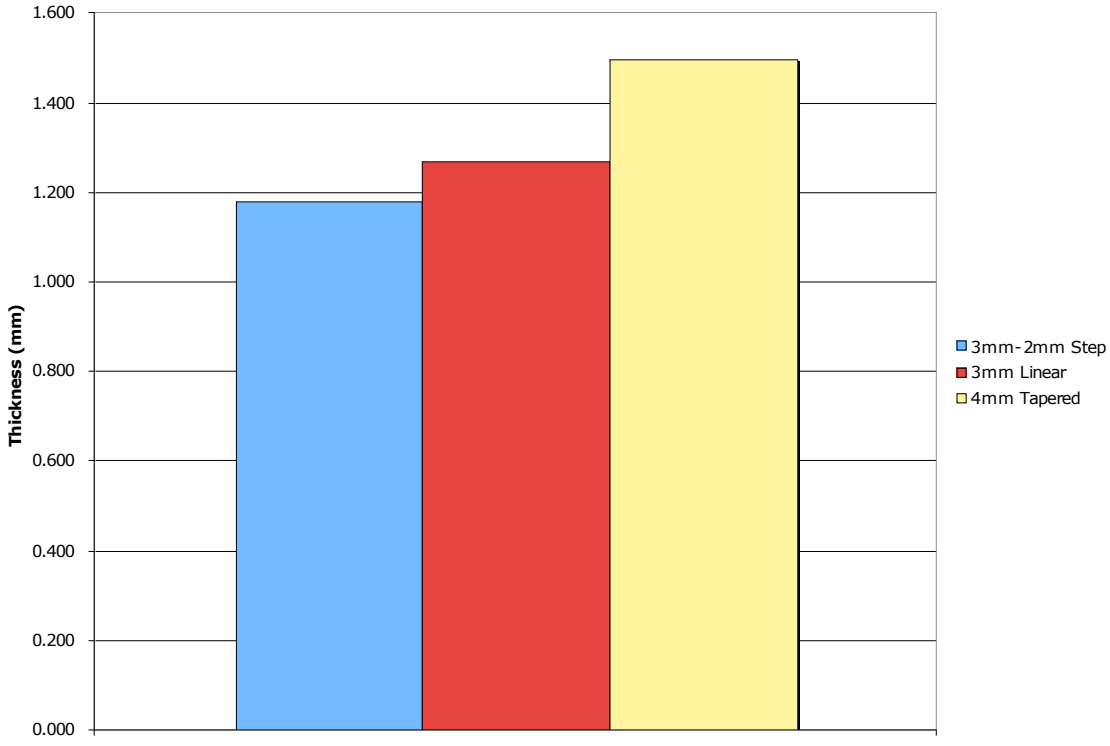

Figure 5.9 – Tapered Hole vs. 3mm Linear Control

Mold geometrical parameters have a large effect on the thickness of the sheet. As can be seen in Figure 5.2, the change between a 1 mm hole and a 3 mm hole more than doubles the thickness of the sheet. However, there are limitations. As can be seen in the linear and stepped holes, 4 mm diameter is simply too large. This was overcome by using the conical hole shape which was created using a surface area model. However, the surface area can only be so large before breakthrough is inevitable.

5.2 Molding Process Parameters

Using the initial linear hole molds, another series of tests was run. This time, the variable was the applied vacuum level. Since the previous tests were completed using 15 inches Hg, an ideal level, they were used as the control. The new tests were measured at a drastically different level – 5 inches of Hg – to identify the effects. The results of the change in vacuum pressure can be seen in Figure 5.10.

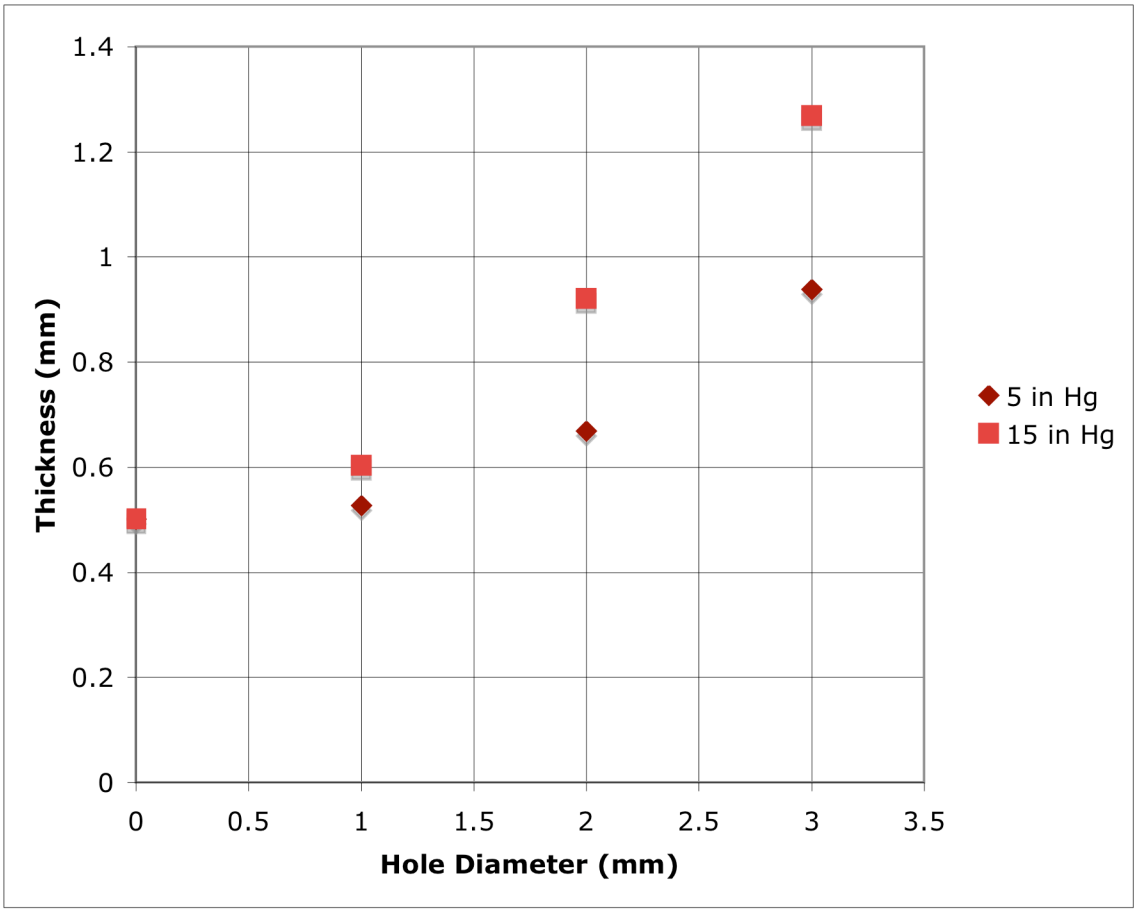

Figure 5.10 – Hole Diameter vs. Thickness for Varied Pressures

Another process parametric consideration in the experiments was the method of drying the samples after the shaping process. In all previous experiments, after the VTH molding, the sample was carefully removed from the mold and placed in the oven to fully dry. There was a thought that perhaps if the samples were dried in the mold, this would prevent shrinkage and produce thicker sheets. However, after completing testing on this idea, it was found to have a negligible effect on the thickness.

These process parameters had a lesser effect on the final sheet thickness than did the mold geometrical parameters. Reducing the vacuum pressure level did have a significant effect on the thickness. Drying the sheets while keeping them in the mold had a negligible effect.

5.3 Paper Parameters

Another condition that was investigated was a paper variable – lower initial moisture content via pre-drying. To get a background for pre-drying, a series of samples were weighed at three times: after being formed, after being molded on the VTH, and fully dried. As can be seen in Table 5.1, after being formed, the samples are about 9% solids. After being molded, they are about 12% solids.

Table 5.1 – Sample Weights

Just Formed Sample Weights (g)	
1.018	
1.144	
1.042	
1.092	
1.074	Average
8.7%	% Solids

Just Molded Sample Weights (g)	
0.791	
0.765	
0.799	
0.898	
0.81325	Average
11.5%	% Solids

Fully Dried Sample Weights (g)	
0.091	
0.089	
0.093	
0.103	
0.091	
0.094	
0.0935	Average

Comparing these results with industrial standards, it was decided to pre-dry a set of samples to 20% solids before molding. It was decided to run these tests on the 2mm linear mold. The linear molds are the most basic and the 2mm mold is the most distinct without any pinholes or breakthrough. First, a series of tests were run to determine the settings for the VTH to achieve 20% solids. These settings were found to be 4.3 in Hg and a dwell time of 500 ms.

To pre-dry the samples, they were created as usual on the British hand sheet former. From there, the sample (still on the forming fabric) was placed on the VTH head face up. Using the settings above, the sheet was pre-dried. Then the sheet was placed face down on the 2mm mold and molded as usual. Thicknesses from these tests compared with the non-pre-dried 2mm linear thicknesses can be seen in Figure 5.11.

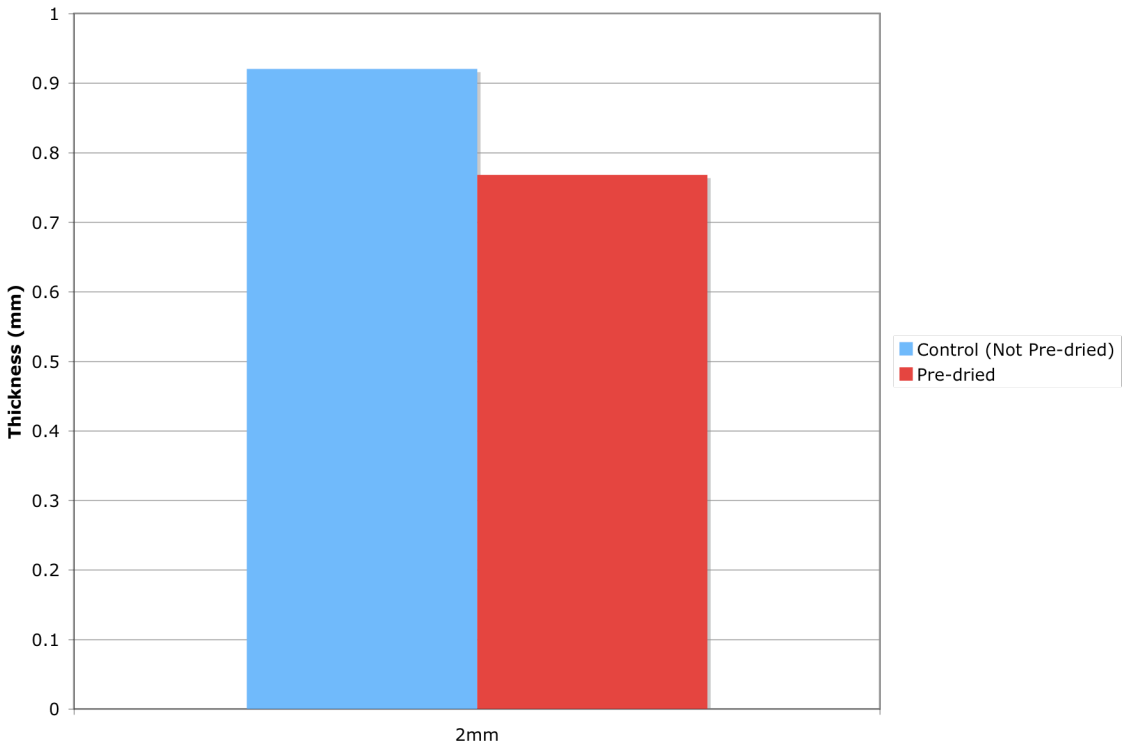

Figure 5.11 – 2mm Thicknesses – Pre-dried and Not Pre-dried

From analyzing these results, it can easily be seen that the pre-dried sheets are not as thick as the samples that were not pre-dried. This led back to the idea of the 4mm diameter holes. As discussed before, both the 4mm straight holes and the 4mm stepped to 3 mm holes had complete breakthrough. Perhaps by using pre-drying, sheets could be created using the 4 mm molds that did not breakthrough. Using the same parameters as the pre-drying example above, sheets were pre-dried to 20% solids and were then tested on both the 4 mm linear holes and the 4 mm stepped holes. Unfortunately, even with the pre-drying, there was still complete breakthrough with the sheets.

Pre-drying certainly had a large effect on the 2mm hole tests. The pre-dried samples had a noticeably smaller thickness than the control samples. However, when pre-drying was used to try to overcome the limitations with the 4 mm molds, there was no visible effect.

5.4 Comparison of Experimental Results with Mathematical Model

There were three major assumptions for the mathematical model: (1) the load is axisymmetrical, (2) the wet web is isotropic and homogenous, and (3) the wet web can be considered a circular plate. As can be shown in the diagram in Figure 5.12, the pressure load was uniform and axisymmetric. Paper is not technically an isotropic, homogenous continuum. It is made up of fibers, water, as well as other chemical compounds. This pulp contained kymene. Assuming that the pulp has been evenly mixed in the formation process, the web can be assumed homogenous. Many other materials, such as metals and polymers are assumed to be isotropic homogenous continua although they are made up of masses of crystals and voids[17]. As all mold geometries were based upon circular holes, the circular model certainly agrees. A thin plate can be defined as an initially flat or curved structural element with a small thickness compared to the remaining dimensions[15]. For these reasons, the model should be adequate for this research. However it is doubtful whether the flexural rigidity of a wet paper web is really constant. It would be expected to depend on the moisture content.

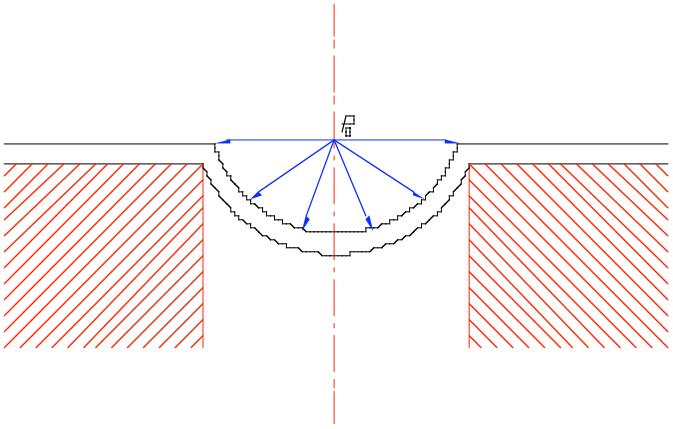

Figure 5.12 – Model of Sheet Showing Uniform Axisymmetric Pressure

To begin, the boundary conditions are chosen. Since the paper web is supported around the hole, but not clamped, simply supported edge boundary conditions will be used from Equation 4.9. Coupling this with Equation 4.8, listed below,

$$\frac{D}{p_o}w = \frac{r^4}{64} + \frac{c_1 r^2}{4}(\ln r - 1) + \frac{c_2 r^2}{4} + c_3 \ln 4 + c_4,$$

the c values are found. Since the equation will give an infinite displacement at r = 0 (the center of the plate) for all values of c_1 and c_3 not equal to zero, c_1 and c_3 must equal zero. Satisfying the boundary condition of w = 0,

$$c_2 = \frac{-a^2}{8} \qquad \text{Equation 5.1}$$

$$c_4 = \frac{a^4}{64} \qquad \text{Equation 5.2}$$

Substituting back into Equation 4.8 with r = 0, this then gives a deflection of:

$$w = \frac{p_o}{64D}\left(a^2 - r^2\right)^2 = \frac{p_o a^4}{64D} \qquad \text{Equation 5.3}$$

Using Equation 4.4 for D, the deflection becomes:

$$w_{\max} = \frac{3p_o a^4 \left(1-\nu^2\right)}{16Et^3} \qquad \text{Equation 5.4}$$

Where,

$$E = \frac{\sigma}{\varepsilon} \qquad \text{Equation 5.5}$$

$$\nu = \frac{-\varepsilon_z}{\varepsilon_x} \qquad \text{Equation 5.6}$$

$w_{max} \cong$ (total thickness – thickness of flat sheet)

$t \cong$ thickness of flat sheet

Both the Modulus of Elasticity and the Poisson's ratios are unknowns for wet paper webs. All other values are known. So to calculate a Modulus of Elasticity for the experimental results, a Poisson's ratio of 0.3 was assumed and the equation was modified to solve for E:

$$E = \frac{3p_o a^4 \left(1-\nu^2\right)}{16wt^3} \qquad \text{Equation 5.7}$$

Utilizing Equation 5.7, values for the Modulus of Elasticity were calculated for 1mm, 2mm, and 3mm linear-holed test sheets at two pressures. These values can be seen in Table 5.2.

Table 5.2 – Modula of Elasticity for Two Pressure Values

	Modulus of Elasticity (Pa)	
Radius (mm)	5 in Hg	15 in Hg
0.5	42300	57100
1	163800	136800
1.5	452900	265200

Investigating these values, the values for the 1.5 mm radius are about 7.5 times bigger than those for the values of the 0.5 mm radius. One of the assumptions for utilizing this model was the deflection was small in comparison with the thickness of the plate. The thickness of the sheet was measured at 0.502 mm. The deflections for these experimental results can be seen in Table 5.3.

Table 5.3 – Deflection Values for Two Pressure Values

	Deflection (mm)	
Radius (mm)	5 in Hg	15 in Hg
0.5	0.025	0.101
1	0.167	0.419
1.5	0.436	0.768

At least one value is larger than the 0.502 mm thickness, and two other values are fairly close. This leads to exploration for another model.

A more extensive model was found in *Roark's Formulas for Stress and Strain*[18]. This model is not limited to small deflections, and should be used whenever the maximum deflection exceeds half the thickness. The equation for the deflection is:

$$\frac{p_o a^4}{Et^4} = K_1 \frac{w}{t} + K_2 \left(\frac{w}{t}\right)^3 \qquad \text{Equation 5.8}$$

Where K_1 and K_2 are based upon the boundary conditions. Using a simply supported model as before,

$$K_1 = \frac{1.016}{1-\nu} \qquad \text{Equation 5.9}$$

$$K_2 = 0.376 \qquad \text{Equation 5.10}$$

Substituting these values into the equation and solving for E yields Equation 5.11.

$$E = \frac{pa^4(1-\nu)}{1.016wt^3 + 0.376w^3t(1-\nu)} \qquad \text{Equation 5.11}$$

Utilizing this equation for the experimental data yields the Modula of Elasticity shown in Table 5.4.

Table 5.4 – Modula of Elasticity Calculated Using Roark's Equation

	Modulus of Elasticity (Pa)	
Radius (m)	16934.165	50802.495
0.0005	230400	168900
0.001	536900	559100
0.0015	895900	1136700

These values do not have as large of a spread as the results using the previous equation. However, there is still an increase in value as the radius increases.

Unfortunately there is limited data about the Modulus of Elasticity for paper in general, especially wet paper webs. However, a few stress-strain curves were found. In Figure 5.13, the stress-strain curve for bleached, dried softwood is presented. This is comparable to the pulp used in the experiments, however this pulp is fully dried.

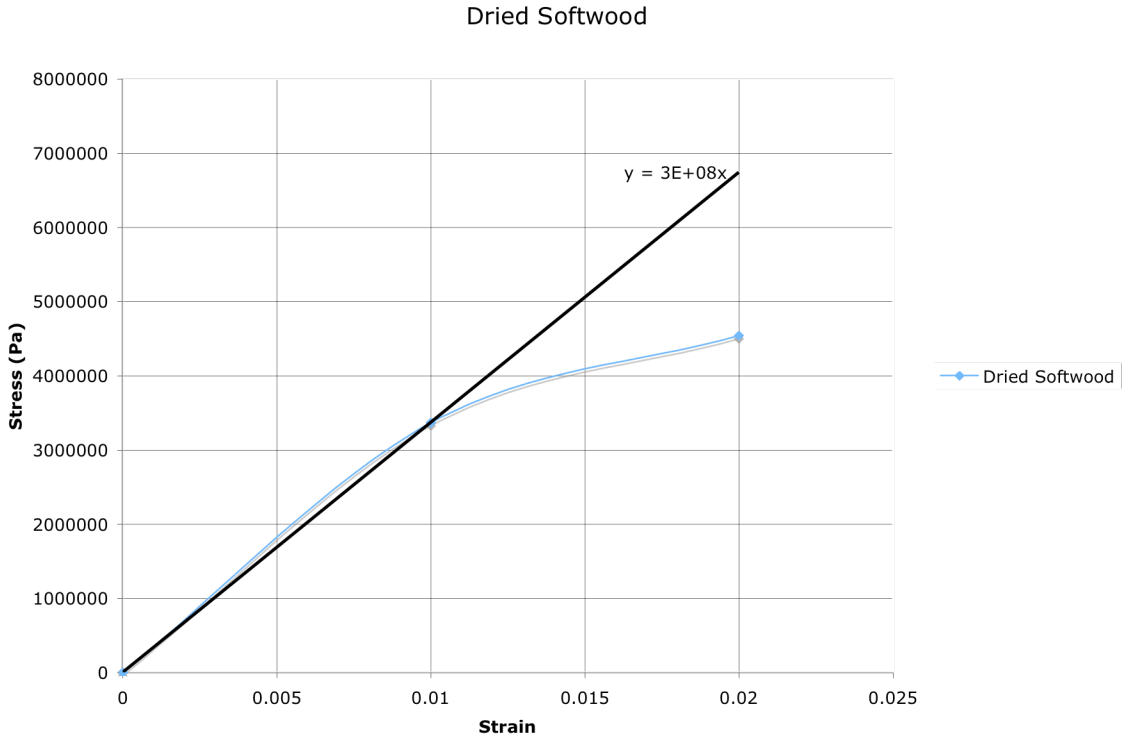

Figure 5.13 – Stress-Strain Curve for Dried Softwood[19]

The trendline is only calculating the slope for the initial (or elastic) portion of the curve. The equation for the trendline is $y = 3x10^8x$. This means that the Modulus of Elasticity for dried softwood is equal to $3x10^8$ Pa. This is much higher than the experimental values obtained using Roark's formula, however, this paper has been fully dried, therefore making it less elastic and yielding a larger Modulus of Elasticity.

The next chart, shown in Figure 5.14, is the stress-strain curve for a handsheet with a solids content of 44.7%. This again is a comparable pulp to the experimental. However, it still has a much higher solids content. The experimental results had a solids content of ~9%.

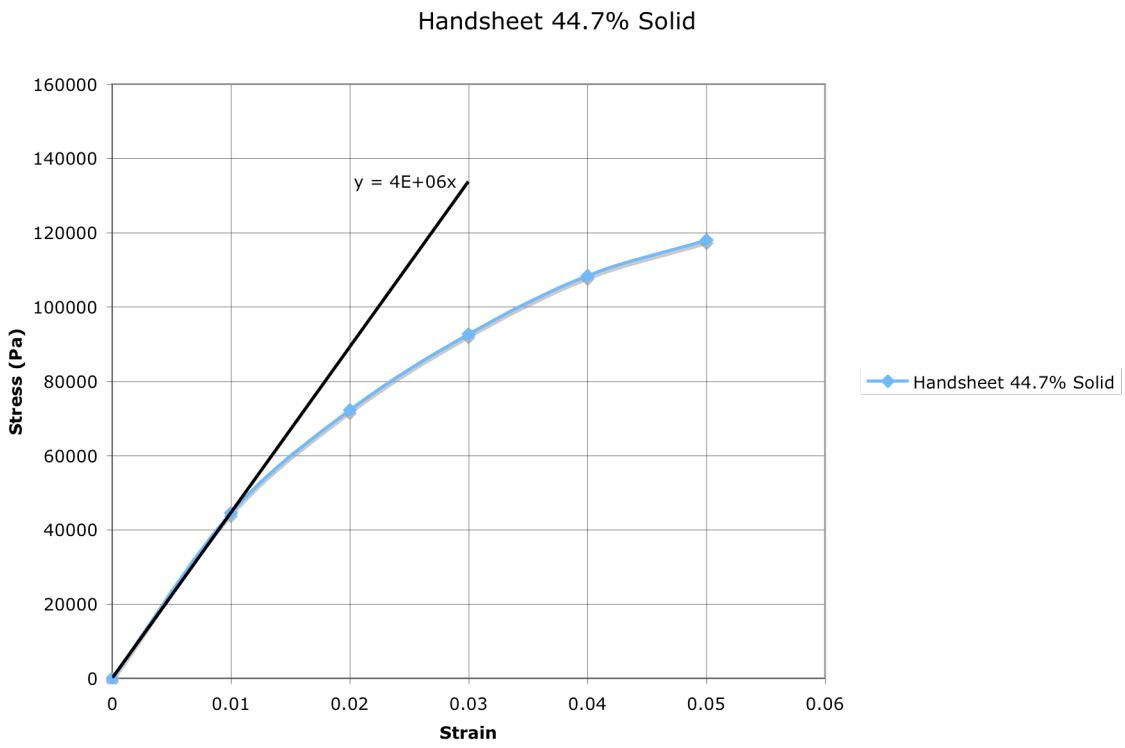

Figure 5.14 – Stress-Strain Curve for 44.7% Solids Handsheet[20]

The slope of the trendline for this curve is $4x10^6$. This is much less than the Modulus of Elasticity for the fully dried paper. Because these handsheets have more moisture, they are more elastic, and therefore have a higher Modulus of Elasticity. Finally, curves were generated using results of groundwood at 21% and 12% solids content. This graph can be seen in Figure 5.15.

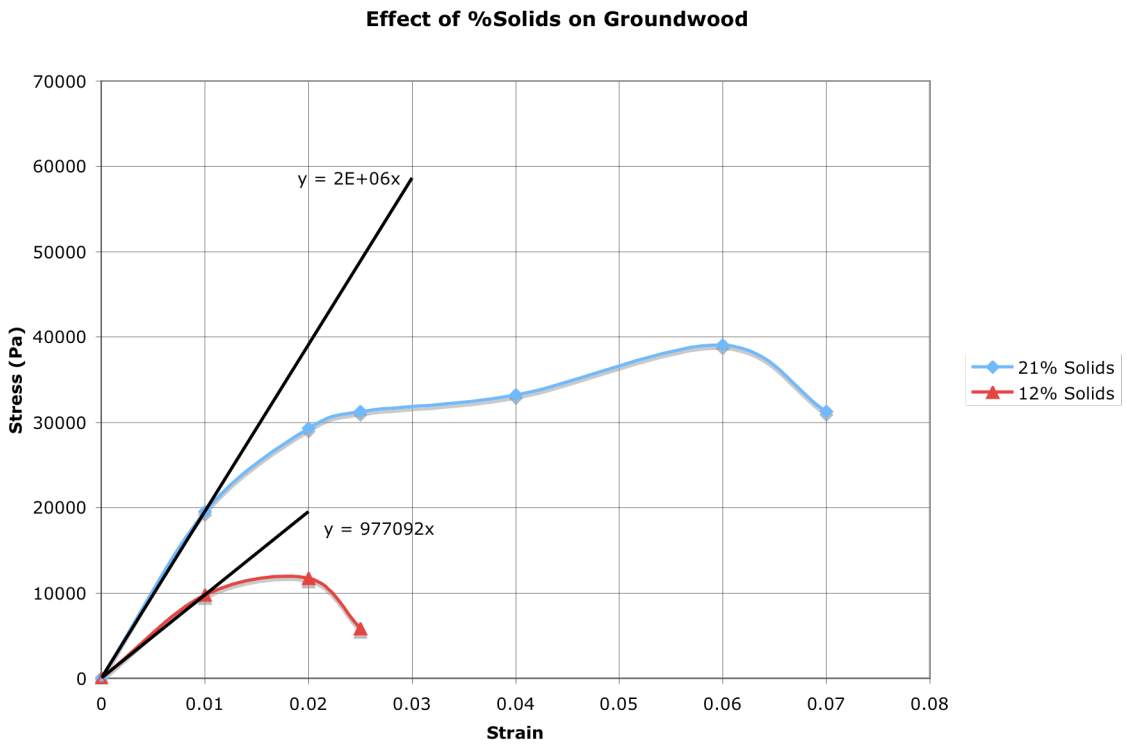

Figure 5.15 – Stress-Strain Curve for Groundwood[21]

Unfortunately, groundwood is a different type of pulp than was used for the experimental results. As the name implies, the pulp is ground, therefore breaking apart the fibers more than in the experimental pulp. This would suggest the experimental pulp would have longer fiber length and therefore a higher Modulus of Elasticity. Also the basis weight of the groundwood samples was not noted in the text, so the comparison is not directly accurate.

The trendlines give a Modulus of Elasticity of 977,092 for the 12% solids and $2x10^6$ for the 21% solids. In section 5.3, results were discussed for two sets of samples – control

(~9% solids) and pre-dried (~20% solids). Using that data and Roark's formula, Modula of Elasticity were calculated for the two cases. These results can be seen in Table 5.5.

Table 5.5 – Modula of Elasticity for Pre-dried vs. Control Samples

	2mm Diameter Holes	
	Control	Pre-dried
E (Pa)	559100	966900

The Modulus of Elasticity for the Pre-dried samples of approximately 20% solids was 966,900 Pa compared with 2,000,000 Pa for the 21% solids groundwood. For the 9% solids control samples, the Modulus of Elasticity was 559,100 Pa compared with 977,092. Certainly these numbers are not exact, but they are not unreasonably different. As mentioned before, the pulp in both experiments is different and the basis weight is not given for the figure. Utilization of the basis weight could have changed the results. The figure as shown in the article, showed stress in g/cm. Aside from changing the units, to get the stress values in pascals, the values were divided by a thickness value. Since neither a thickness, nor a basis weight was given in the text, the values were divided by the experimental thickness of 0.5 mm.

A final inconsistency with the experimental calculation is the Poisson's ratio. As mentioned previously, a value of 0.3 was assumed to calculate the Modulus of Elasticity. Apart from that value being an assumption, unlike most materials, paper does not hold a constant Poisson's ratio. Paper often demonstrates a straightening anomaly. As a fiber undergoes wet straining, it tends to straighten, pushing the fibers crossing it apart[22]. This

causes an increase in caliper, which can often be so much that the Poisson's ratio actually becomes a negative value. This could explain the variation of the E values in Table 5.4.

To compare the experimental deflections with a generated radius/deflection curve, an average Modulus of Elasticity of 547,978 Pascals was calculated utilizing the average of the 0.001m radius Modulus of Elasticity values from Table 5.4. This comparison can be seen in Figure 5.16.

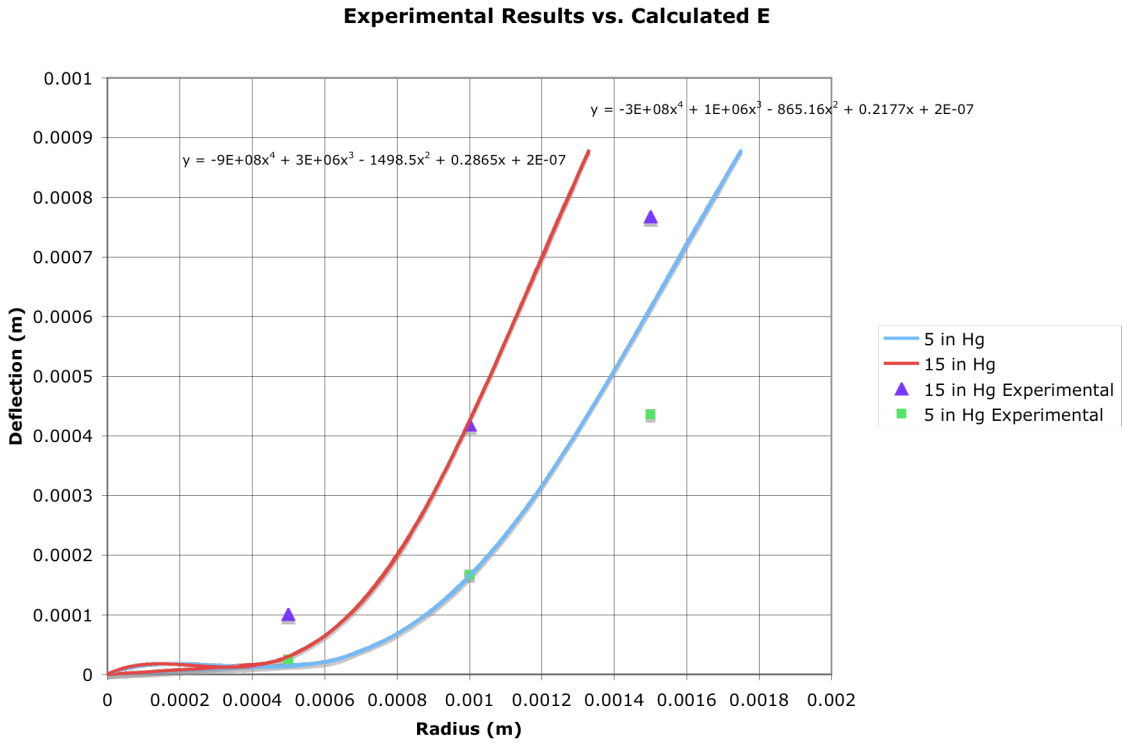

Figure 5.16 – Experimental Results compared to Radius/Deflection Curve

The data points measured experimentally reasonably fit the radius deflection curve, showing that utilization of the mathematical model, and more specifically, Roark's equation, can generate a Modulus of Elasticity that is reasonable. As Figure 5.16 shows,

the relationship between the radius (a) and the deflection (w) is not a simple a^4/w relationship as the initial mathematical model suggested. The Modula of Elasticity generated utilizing the experimental data were comparable and in the same range as those found in Figures 5.13-5.15. However, paper is more complicated than traditional metal and polymer materials, and the mathematical model is too simple to generate a truly accurate result. A complete comparison of the Modula of Elasticity can be found in Table 5.6.

Table 5.6 – Complete Comparison of Modula of Elasticity

Type	Pressure (in Hg)	Modulus of Elasticity (Pa)
1mm Diameter	5 in Hg	230400
1mm Diameter	15 in Hg	168900
2mm Diameter	5 in Hg	536900
2mm Diameter	15 in Hg	559100
2mm Diameter Predried to 20% Solid	15 in Hg	966900
3mm Diameter	5 in Hg	895800
3mm Diameter	15 in Hg	1136700
Groundwood 12% Solids	n/a	977092
Groundwood 21% Solids	n/a	2000000
Handsheet 44.7% Solids	n/a	4000000
Dried Bleached Softwood	n/a	300000000

6 CONCLUSIONS AND RECOMMENDATIONS FOR FUTURE WORK

In summary, all the variables have some effect on the final paper sample. Geometrical parameters seem to have the most effect. Increasing the hole size, to a certain limit, increases the thickness of the sheet. Changing the geometry was also a large factor, as changing the geometry of the hole to a taper allowed a 4mm diameter hole to form a dome, creating a sheet thicker than any sheets created from the straight holes. Use of the "simplified mold geometries" (versus the more complex industrial fabrics) made it easier to investigate the geometry variables.

Another geometrical parameter that could be researched is the hole spacing. It seems there would be a negative effect on the thickness if the holes were spaced too closely together. The hole spacing was not varied in the tests, therefore there was no indication of any effect, and really no concrete method of testing this theory. In terms of testing, a further recommendation would be revisiting the shadow moiré technique. Certainly some manner of this testing would accommodate a small sample size and generate its topography.

The process and paper parameters also had an effect on the final thickness. Increasing the vacuum pressure increased the sheet thickness, whereas pre-drying the sheet reduced the sheet thickness. These parameters are more subject to industrial protocol. Two other parameters that could be investigated would be the effect of the sheet basis weight

(thickness) and utilizing a flexible membrane over the sheet to reduce pinholes. These parameters coupled with larger diameter holes could potentially produce thicker sheets.

The sheet basis weight is especially interesting with respect to the mathematical model. Recalling Equation 5.8:

$$\frac{p_o a^4}{Et^4} = K_1 \frac{w}{t} + K_2 \left(\frac{w}{t} \right)^3$$

the vacuum (p_o), the radius (a), and the Modulus of Elasticity (E) were all considered throughout the experiments. The thickness (t) refers to the flat sheet thickness, which depends upon the sheet basis weight. Based upon the equation, as the thickness increased, the maximum deflection would decrease, and therefore, as the sheet basis weight increased, the maximum deflection would increase. Further research on this subject could verify this assumption.

This research has indirectly considered the Modulus of Elasticity. By utilization of the experimental results and Roark's equation, a Modulus of Elasticity could be calculated for each variable. This showed varied E values depending upon the hole diameter which illustrates the idea that paper does not behave like a typical metal or polymer. Especially with consideration to the phenomenon of paper increasing in thickness as stretching occurs, this research has shown that a more sophisticated mathematical model is needed to accurately determine the Modulus of Elasticity for wet paper webs.

REFERENCES

[1] Kamps, Richard Joseph, et al., 2001. *Decorative Formation of Tissue.* United States Patent 6,203,663.

[2] Hada, Frank S., et al., 2005. *Through-Air Dryer Assembly.* United States Patent 6,877,246.

[3] TAD - Thru-Air Drying. 2006. Metso Paper, Inc. < http://www.metsopaper.com/paper/MPwHome.nsf/FR?ReadForm&ATL=/paper/MPwTissue.nsf/WebWID/WTB-041125-2256F-E9A25>. February 2006.

[4] Trokhan, Paul Dennis and Vitenberg, Vladimir. 1999. *Method of Making Paper Web Using Flexible Sheet of Material.* United States Patent 5,893,965.

[5] Lindsay, Jeffrey Dean, et al., 2006. *Methods of Making a Three-Dimensional Web.* United States Patent 6,998,017.

[6] Trokhan, Paul D. 1985. *Deflection Member.* United States Patent 4,528,239.

[7] Burazin, Mark Alan, Kai F. Chiu, and Jeffrey Dean Lindsay. 2004. *Absorbent Tissue Products Having Visually Discernable Background Texture.* United States Patent 6,746,570.

[8] Chiu, Kai F., et al., 1995. *Apparatus for Making Soft Tissue Products.* United States Patent 5,429,686.

[9] Rosen, David. "Chapter 3 Introduction." ME7227 Course Notes. 24 August 2004.

[10] "Laboratory Beating of Pulp (Valley Beater Method)" TAPPI. T-200 sp-96.

[11] "Freeness of Pulp." TAPPI. T-227 om-85.

[12] Sammons, Mell Tex. "Vacuum Test Head Operation Procedure." IPST Distribution. 15 December 2004.

[13] Loughran, James. "Caliper for TAD Towel." IPST Distribution. 7 February 2005.

[14] Hojjatie, Barry, and Coffin, Douglas. "Determination of Sheet Topography using Shadow Moiré Method." TAPPI Journal Vol. 4: No.3.

[15] Hojjatie, Barry, and Coffin, Douglas. "Determination of Sheet Topography using Shadow Moiré Method." TAPPI Journal Vol. 4: No.3.

[16] Ugural, A. C., and S. K. Fenster. *Advanced Strength and Applied Elasticity.* New York: Elsevier, 1987.

[17]Carter, Barton P. "Effect of Pore Size and Thickness on Critical Pressure of Elastic Systems" Thesis Georgia Institute of Technology, 2005.

[18] Young, Warren C. *Roark's Formulas for Stress & Strain.* Texas: McGraw-Hill, 1989.

[19] Seth, R.S., and Page, D.H. "The Stress Strain Curve of Paper." The Role of Fundamental Research in Papermaking. Vol. 1: p. 421-452.

[20] McDonald, J.D., Pikulik, I.I., and Daunais, R. "On-Machine Stress-Strain Behaviour of Newsprint." Journal of Pulp and Paper Science Vol. 14: No.3: May 1968.

[21] Mardon, J., Cutshall, K.A., and Laurila, P.S. "The Load Stretch (Wet Web Strength) Behaviour of Selected Paper Pulps and Furnishes." Pulp and Paper Magazine of Canada. Vol. 74: No. 11: November 1973.

[22] Baum, G.A., Pers, K., Shepard, D.R., and Ave'Lallemant, T.R. "Wet Straining of Paper." Tappi Journal. Vol. 7: No. 5.